LEGIBILITY NOTICE

A major purpose of the Technical Information Center is to provide the broadest dissemination possible of information contained in DOE's Research and Development Reports to business, industry, the academic community, and federal, state and local governments.

Although a small portion of this report is not reproducible, it is being made available to expedite the availability of information on the research discussed herein.

ORNL/TM--8977

DE84 016555

Engineering Physics and Mathematics Division

PHASE I MEASUREMENTS FOR THE HTGR BOTTOM REFLECTOR AND CORE SUPPORT BLOCK NEUTRON-STREAMING EXPERIMENT

F. J. Muckenthaler
L. B. Holland*
J. L. Hull*
J. J. Manning

Date of Issue: July 1984

Research sponsored by
U.S. DOE Office of
Converter Reactor Deployment

*Operations Division

Prepared by the
Oak Ridge National Laboratory
Oak Ridge, Tennessee 37831
operated by
Martin Marietta Energy Systems, Inc.
for the
U.S. DEPARTMENT OF ENERGY
under Contract No. DE-AC05-840R21400

CONTENTS

ACKNOWLEDGEMENTS

The author is grateful for the assistance of Dr. D. T. Ingersoll in the formulation of the Experimental Program Plan and for his coordination of the procurement and fabrication of the experimental components. The participation and cooperation of Dr. D. E. Bartine, Program Manager, and GA Technologies in this effort are also appreciated. Special thanks go to J. O. Johnson, The University of Tennessee, for reduction of the hydrogen counter data and to Lorraine Abbott, Sue R. Damewood and Stephanie A. Raby, all of ORNL, for their efforts in the editing and preparation of this report.

PHASE I MEASUREMENTS FOR THE HTGR BOTTOM REFLECTOR AND CORE SUPPORT BLOCK NEUTRON-STREAMING EXPERIMENT

ABSTRACT

This report presents the Phase I measurements of the High-Temperature Gas-Cooled Reactor Bottom Reflector and Core Support Neutron Streaming Experiment conducted at the ORNL Tower Shielding Facility during FY-1983. In this phase the first four of eight segments that comprise the full experimental mockup were utilized. These were (1) an upper boron pin layer (graphite matrix) followed by a boral shroud, (2) a graphite reflector layer, (3) a graphite coolant crossover layer, and (4) a graphite follow-on layer, all containing coolant holes. A collimated beam from the Tower Shielding Reactor II was used as the neutron source. In order to obtain a spectrum of neutrons more nearly like the spectrum expected from the HTGR, an iron and graphite spectrum modifier was inserted in the TSR-II beam ahead of the experimental mockup. The various experimental configurations tested resulted from the successive addition of the four graphite layers to the mockup. Neutron energy spectra were measured behind the spectrum modifier and the boron pin layer and integral neutron fluxes were measured behind the spectrum modifier and behind each of the four layers. The measurements were divided into two parts, the two parts differing in the composition of the boron pin layer. During Part I, a reference pin pattern was used which consisted of a combination of graphite and boronated graphite pins. During Part II, a full pattern of boronated graphite pins was used. The experimental data are presented in both tabular and graphical form.

1. INTRODUCTION

During FY-1983, a series of measurements were performed at Oak Ridge National Laboratory's Tower Shielding Facility to provide data for the verification of the calculational methods used to predict the transport of radiation through the bottom reflector and core support structure of General Atomic Company's current design of the High Temperature Gas-Cooled Reactor (HTGR). The measurements comprised the first phase of a two-phase experimental study and thus have been designated as the Phase I measurements of the HTGR Bottom Reflector and Core Support Block Neutron-Streaming Experiment.

In the HTGR, the principal shielding problem in the bottom reflector and core support block region is the downward streaming of neutrons from the reactor inside the lower plenum through the many coolant holes that penetrate the region. In an attempt to inhibit the neutron streaming through these holes, the HTGR design specifies that two regions of the bottom reflector contain boron in the form of boronated graphite pins inserted into small holes drilled in the reflector's graphite matrix. One boron pin region lies directly below the core in a part of the reflector that contains numerous small coolant holes, while the other is located in a lower portion of the reflector in which the small coolant holes have merged into six large coolant holes.

The Phase I measurements reported on here were designed both to determine the extent of neutron streaming through the upper portion of the bottom reflector and to investigate the effectiveness of the

upper boron pin region in reducing the streaming. For these measurements, an experimental configuration was fabricated which consisted of four segments identified as (1) an upper boron pin layer, (2) a reflector layer, (3) a crossover layer, and (4) a follow-on layer, all containing simulated coolant holes.

The experiment was divided into two parts, the two parts differing in the pattern of "pins" used in the upper boron pin layer. During the Part I measurements, nearly equal numbers of boronated graphite pins and plain graphite pins were inserted in the layer in a pattern identified as the reference pattern. During the Part II measurements, only boronated graphite pins were used, and the pattern was referred to as the full pattern.

The experimental configuration was positioned in a horizontal beam emerging from the Tower Shielding Reactor II (TSR-II). Preceding the configuration in the beam were slabs of iron and graphite that modified the TSR-II neutron spectrum to more nearly resemble the neutron spectrum emerging from the bottom of the HTGR core. These slabs are referred to as the "spectrum modifier."

The relative effectiveness of the two pin patterns in reducing neutron streaming was investigated by performing both integral neutron-flux measurements and fast-neutron spectral measurements behind the two boron pin layers, as well as behind the spectrum modifier. Further streaming through the mockup was investigated through integral measurements behind each of the successive layers of the mockup as they were added to the experimental configuration. The integral measurements were made with the Bonner ball detector system developed at the TSF, and the spectral measurements were made with an NE213 liquid scintillator spectrometer and hydrogen-filled proton-recoil counters.

In the Phase II measurements, which will be completed in FY 1984, four additional segments will be added to the mockup, including a segment representing the lower boron pin layer.

2. INSTRUMENTATION

The TSF Bonner ball detection system consists of a series of detectors (balls), each of which measures an integral of the neutron flux weighted by the energy-dependent response function for that ball. The detection device of a Bonner ball consists of a 5.1-cm-diameter spherical proportional counter filled with BF_3 gas ($^{10}B/B$ concentration = 0.96) to a pressure of 0.5 atmospheres. In order to cover a range of neutron energies, the counter is used bare, covered with cadmium, or enclosed in various thicknesses of polyethylene shells surrounded by cadmium, each detector being identified by the diameter of its shell. Bonner ball experimental results are predicted analytically by folding a calculated neutron spectrum with the Bonner ball response functions determined by Maerker et al.[1] and by C. E. Burgart et al.[2]

The NE213 liquid scintillator spectrometer covered the neutron spectral region from about 800 keV to 15 MeV. The pulse-height data obtained with the spectrometer were unfolded with the FERD code[3] to yield absolute neutron energy spectra.

The spherical proton-recoil counters, filled with hydrogen to pressures of 1, 3, and 10 atmospheres, covered the neutron energy range from about 50 keV to 1 MeV. Pulse-height data from the counters were unfolded with the SPEC-4 code,[4] which uses the unfolded NE213 neutron spectrum for the high-energy input.

The measurements for each detector were referenced to the reactor power (watts) using as a basis the data from two fission chambers positioned along the reactor centerline. The response of these chambers as a function of reactor power level was established previously through several calorimetric measurements of the heat generated in the reactor during a temperature equilibrium condition (heat-power run).

3. EXPERIMENTAL CONFIGURATIONS

The experimental program plan (see Appendix A) called for neutron measurements to be made behind the graphite segments mocking up the various sections of the HTGR bottom support structure as they were added to the configuration. The source for the measurements was to be the TSR-II; however, as pointed out in the introduction, it was first necessary to modify the spectrum of neutrons emerging from the TSR-II to more nearly resemble the spectrum of neutrons predicted to emerge from the bottom of the HTGR. Preanalysis calculations[5] for the experiment fixed the composition and thickness of the spectrum modifier and contributed to the design of the various graphite segments, all of which are described below.

3.1 SPECTRUM MODIFIER

The preanalysis calculations indicated that 5.1 cm (2 in.) of iron followed by 30.5 cm (12 in.) of graphite placed in the TSR-II beam would provide a spectrum of neutrons representative of those leaving the HTGR core. In the experiment the iron slab (see Fig. 1) was one solid piece 152.4 cm (60 in.) on an edge. The graphite slab was built from pieces that were 10.16 cm (4 in.) on a side and 121.9 cm (48 in.) long and were stacked to make a slab equivalent in width to the iron slab. A listing of the metallic components found in the iron and graphite are given in Tables 1 and 2, respectively. (Note: All tables are included in Appendix B.)

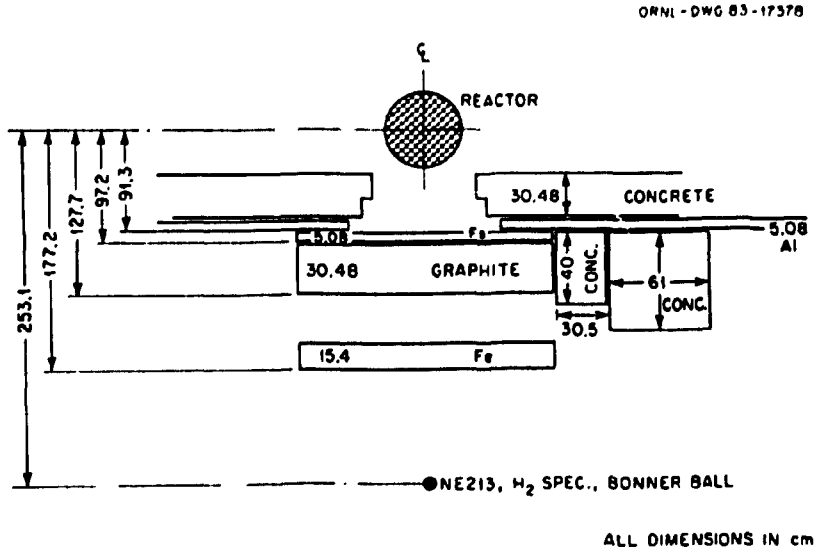

Fig. 1. Schematic of iron and graphite spectrum modifier (SM). Note: Concrete covers lateral sides of configuration.

The spectrum modifier (SM) was surrounded with a 91.5-cm (36-in.) thickness of concrete to minimize the amount of background radiation reaching the detector. The inner 30.5 cm (12 in.) of the concrete consisted of small blocks 15.2 cm on edge and 30.5 cm long (6 in. facing, 12 in. long), and the outer 61 cm consisted of large blocks 61 cm on edge and 30.5 cm thick (24 in. facing, 12 in. thick). The results of chemical analyses of the blocks in the two layers are presented in Tables 3 and 4.

As indicated in Fig. 1, the spectral measurements were made at 125.4 cm beyond the SM. The 15.4-cm-thick iron slab (actually three pieces, each approximately 5 cm thick) shown positioned between the SM and the detector was in place for the spectral measurements to reduce the gamma-ray flux at the detectors.

3.2 UPPER BORON PIN LAYER

The upper boron pin layer consisted of four pieces of graphite 20.3 cm (8 in.) thick and 55.88 cm (22 in.) on a side, each piece containing an identical pattern of 1.27-cm- and 1.588-cm-diameter holes (0.5 and 0.625 in.). When the four pieces were combined, the hole patterns were grouped into seven hexagons, six centered around one. The pieces were surrounded by additional graphite to make the mockup 152.4 cm (60 in.) on a side, as shown in Fig. 2, and the entire layer was then surrounded by concrete as described in Sect. 3.1.

The six outer hexagons were identical, each containing 216 of the smaller (1.27-cm-diameter) holes and 108 of the larger (1.588-cm-diameter) holes. The center hexagon contained the same number of the smaller holes, but only 68 of the larger holes. Thus, the boron pin layer contained a total of 1512 of the smaller holes and a total of 716 of the larger holes.

As mentioned previously, for the Part I measurements, some of the smaller holes (770) were filled with boronated graphite (BG) pins and some (738) were filled with graphite pins. (Four of the small holes accommodated permanent graphite pins as described in the following paragraph.) For the Part II measurements, all the smaller holes (except those containing the four permanent graphite pins) were filled with BG pins. The larger (1.588-cm-diameter) holes represented flow paths for the cooling gas and thus were left open.

The arrangement of BG and graphite pins used in the Part I measurements is referred to as the *reference pattern* and is shown in Fig. 3, where the dark holes represent locations of the BG pins and the small clear circles indicate holes filled with graphite pins. (Figure 3 actually shows only one-fourth of the pin array.) The one hole marked with an X in the partial center hexagon (fifth vertical row from left, third hole from top) identifies the location of one of the four permanent graphite pins, the others being located in corresponding positions in each of the other three pieces of the boron pin layer.

The arrangement of the all-BG pins used in the Part II measurements is referred to as the *full pattern* and is shown in Fig. 4. As noted above, in this pattern all the graphite pins except the four permanent ones were replaced with BG pins.

The BG pins were extruded (by the General Atomic Company) from graphite flour, nuclear grade boron carbide (19.8 at % ^{10}B), and a phenolic binder. Table 5 gives the average properties of the pins as submitted by the vendor, together with the results from two chemical analyses performed at Oak Ridge National Laboratory.

The graphite pins and the graphite matrix in the four segments, supplied by Airco Carbon, were fabricated from grade 873S carbon and had a density of 1.75 g/cc. The results of three ORNL analyses of the graphite are given in Table 6.

ORNL-PHOTO 4110-83

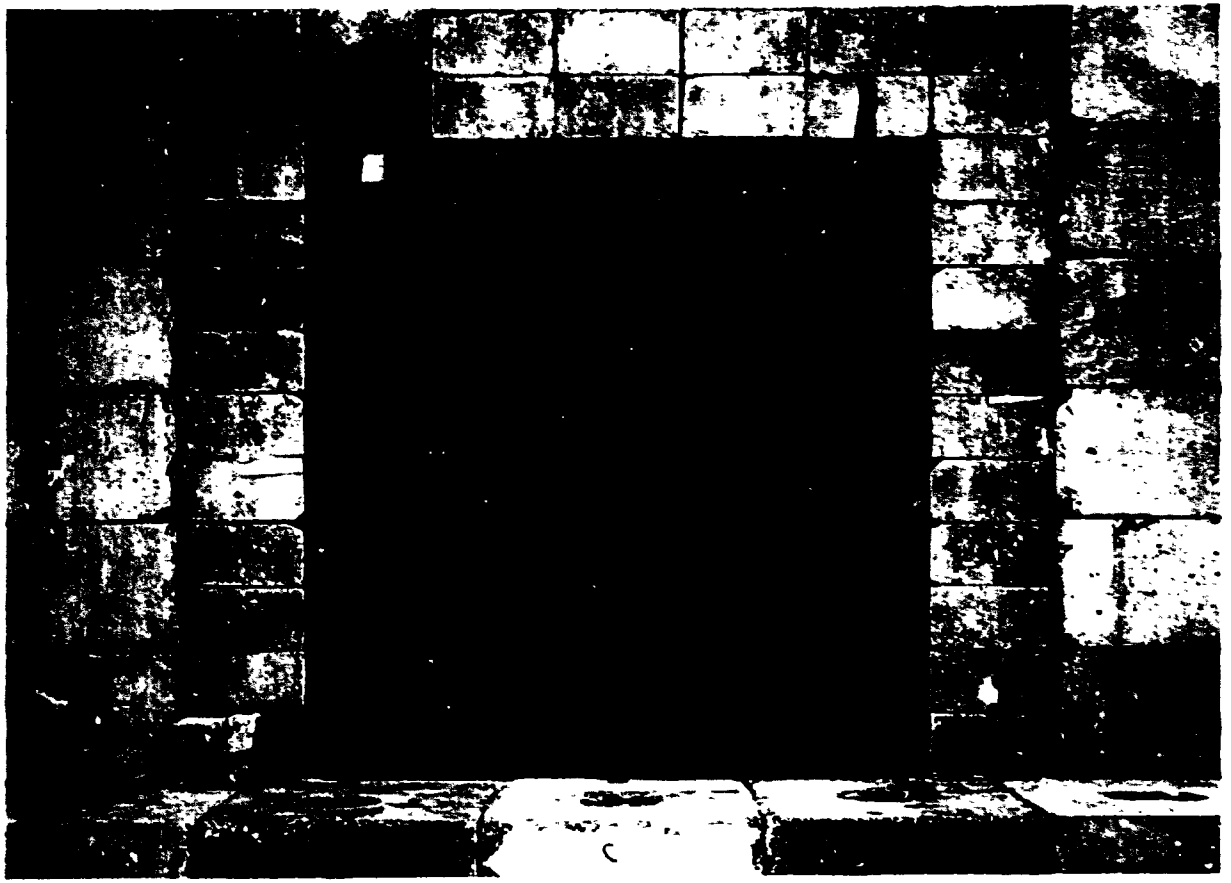

Fig. 2. Photograph of upper boron pin layer (Item II A).

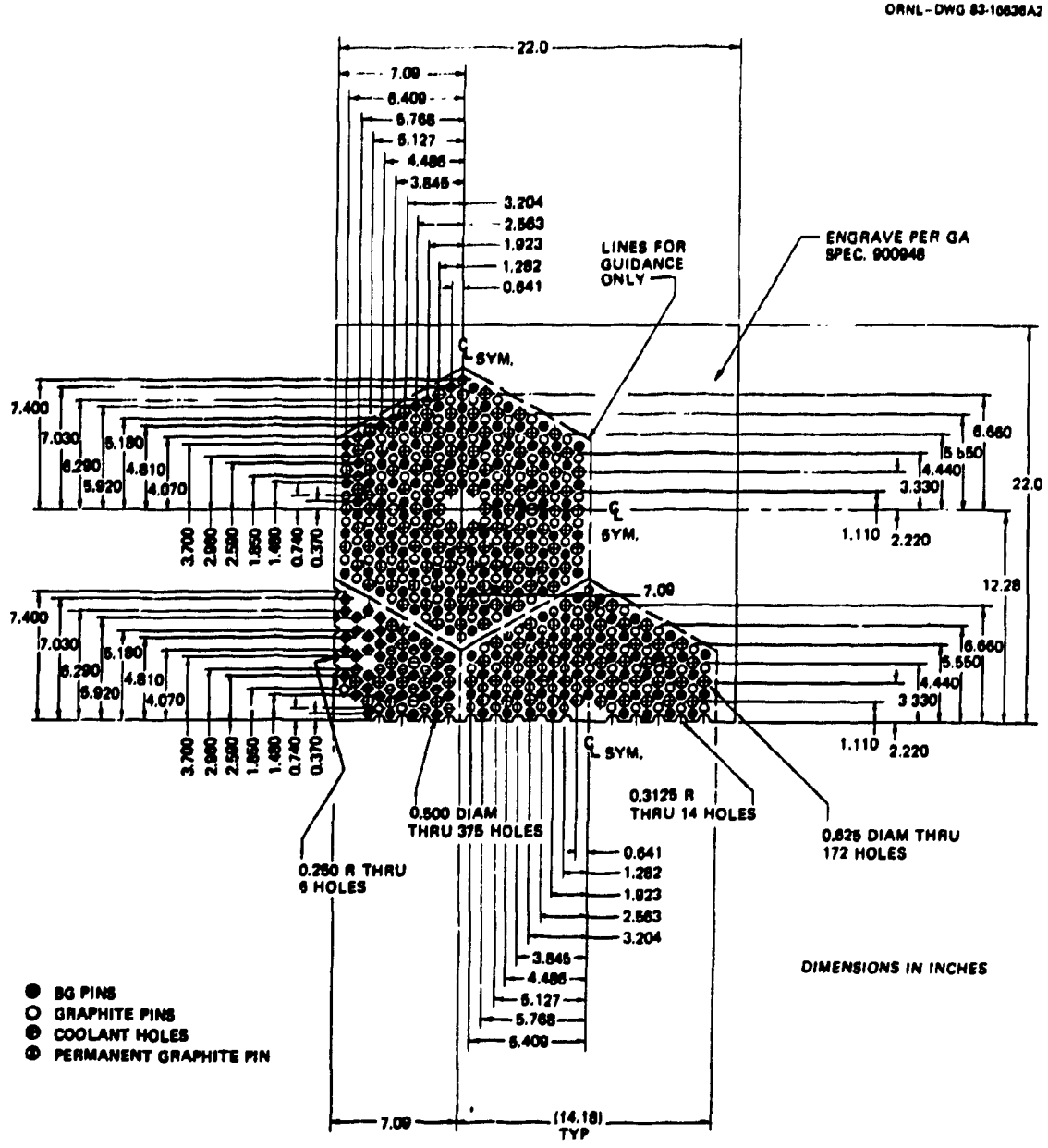

Fig. 3. Sketch of one-fourth of upper boron pin layer containing BG and graphite pins (reference pin pattern) (Item II A).

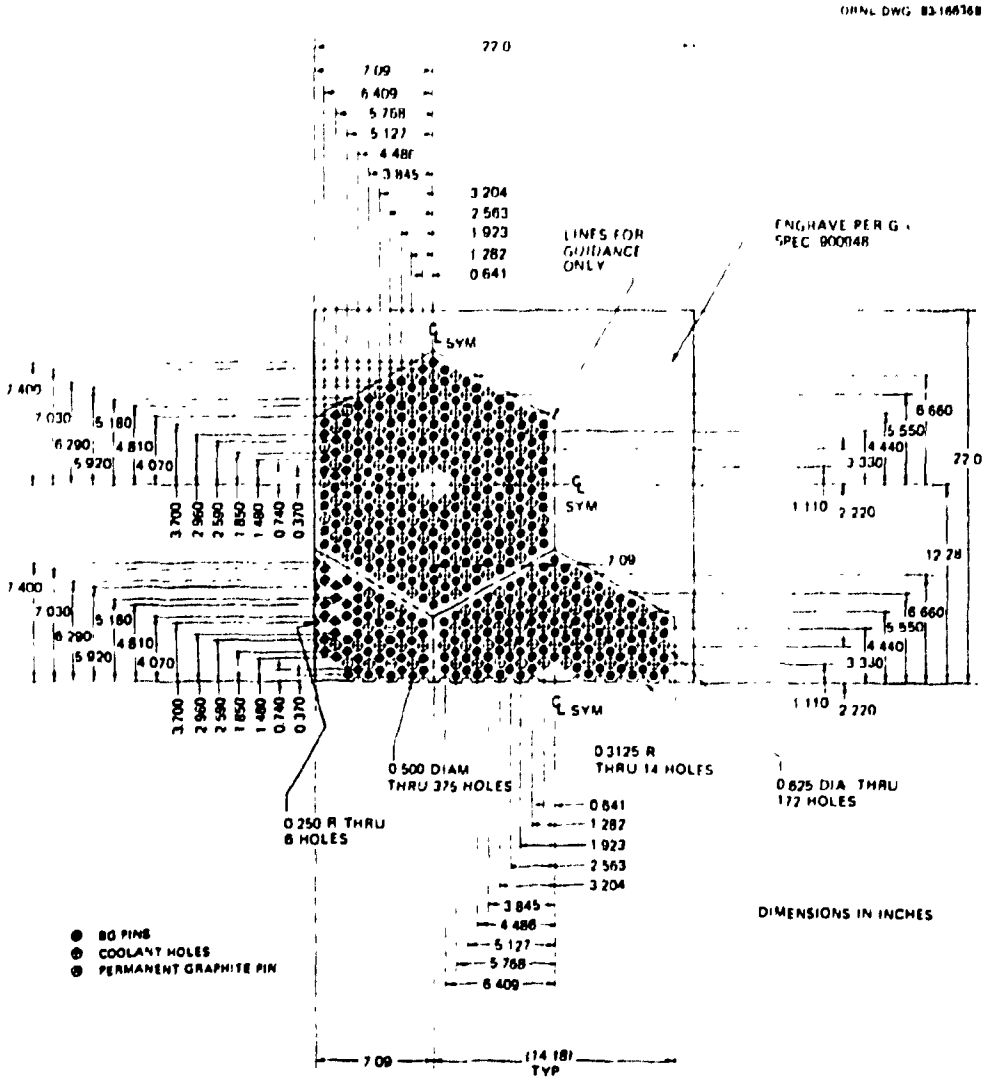

Fig. 4. Sketch of one-fourth of upper boron pin layer containing BG pins only (full pin pattern) (Item III A).

A diagram of the experimental configuration containing both the SM and the boron pin layer is shown in Fig. 5. (The figure also shows the three-piece iron layer placed behind the configuration during the spectral measurements and for one series of 3-, 6-, and 10-in. Bonner ball measurements at the spectrometer location.)

A boral shroud (iris), 0.66 cm thick (0.26 in.) and 152.4 cm on a side, was positioned directly behind the boron pin layer. As shown in Fig. 6, the interior surface of the shroud followed the outline of the seven-hexagon array, so that the pins and coolant holes were exposed to the next segment of the mockup (the reflector layer). The properties of the boral are given in Table 7, and the position of the shroud in the experimental configuration is shown in Fig. 7.

3.3 REFLECTOR LAYER

The reflector layer following the upper boron pin layer and the boral shroud also consisted of four pieces of graphite placed edge on and surrounded by additional rectangular pieces of graphite to form a 22.9-cm-thick (9-in.-thick) by 152.4-cm-square slab whose edges were surrounded by concrete. The layer contained 716 coolant holes whose diameter (1.588 cm) and locations matched those in the preceding boron pin layer. A photograph of the reflector layer in position is shown in Fig. 8, and a schematic of the coolant holes in one of the four pieces of the layer is presented in Fig. 9.

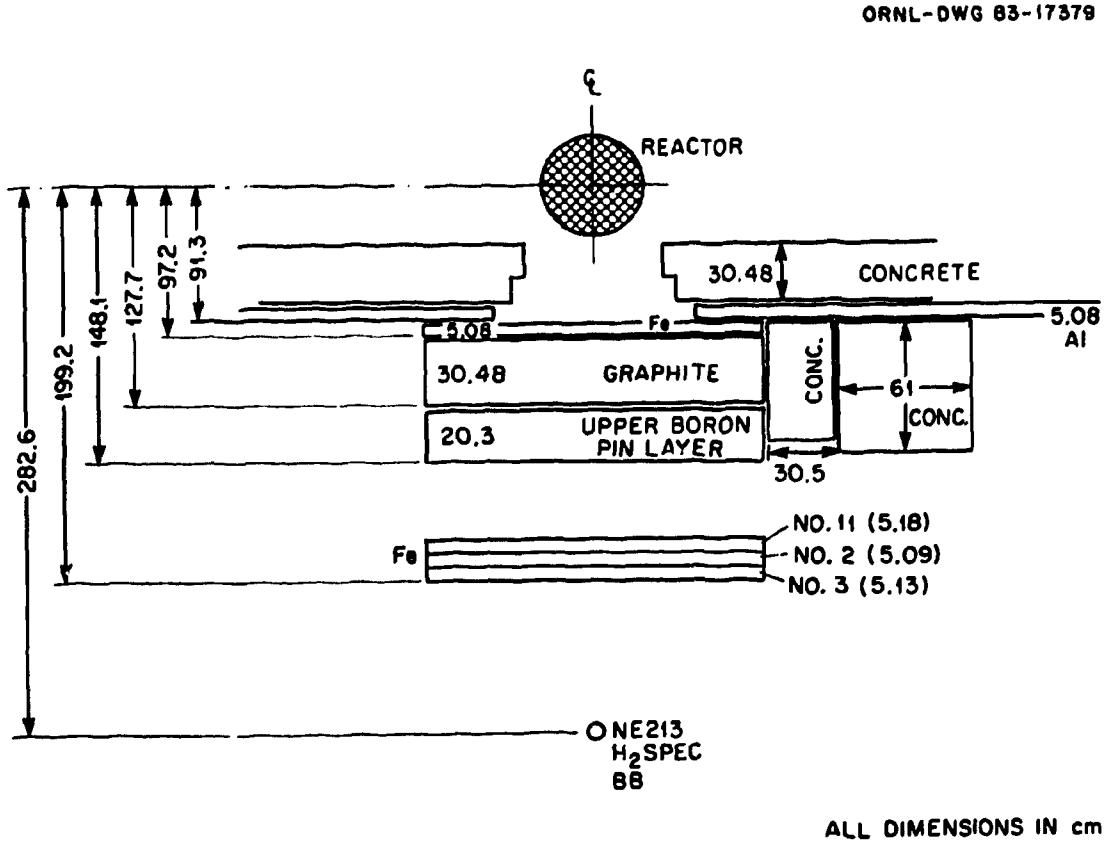

Fig. 5. Schematic of configuration containing SM + upper boron pin layer (Item II A). Note: Concrete covers lateral sides of configuration.

ORNL-PHOTO 3827-83

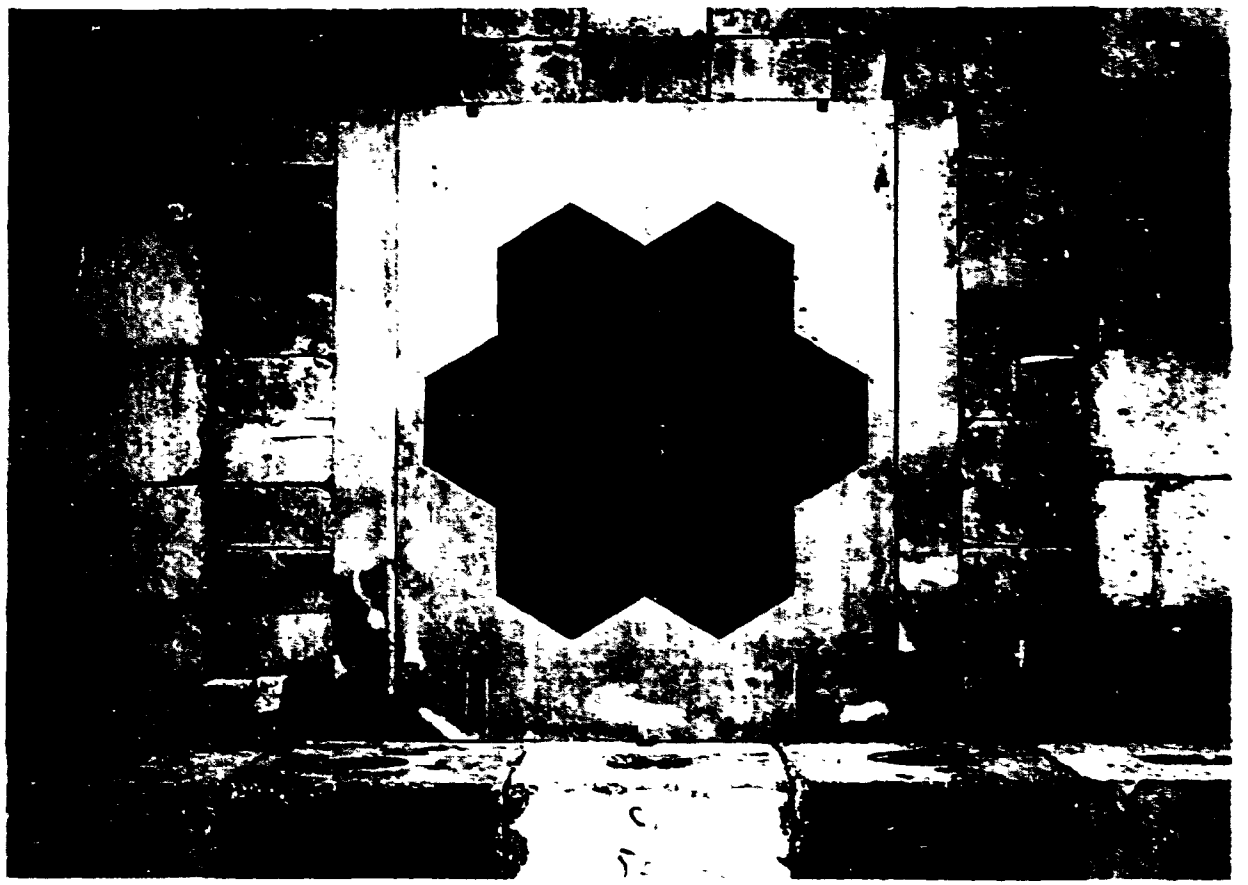

Fig. 6. Photograph of boral shroud (iris) behind upper boron pin layer.

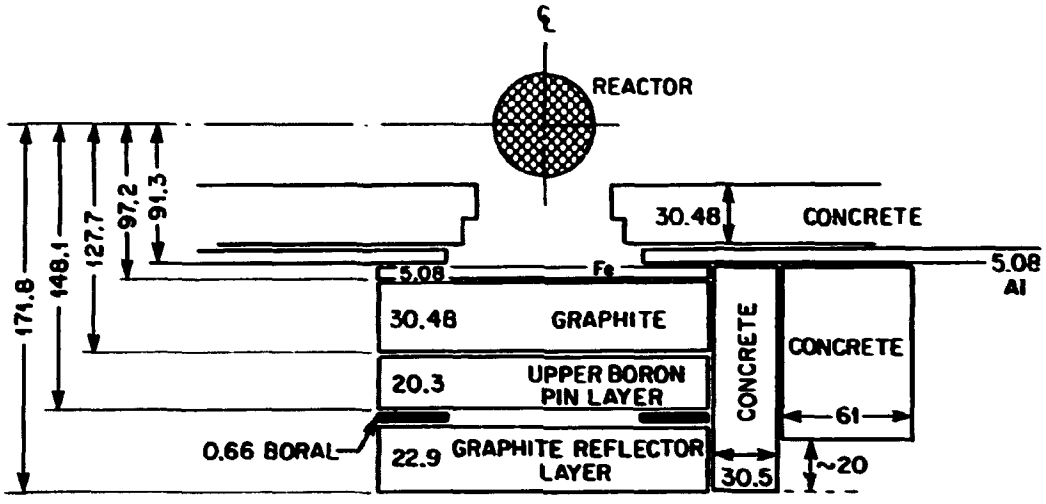

Fig. 7. Schematic of configuration containing SM + upper boron pin layer + boral shroud + reflector layer (Item II B). Note: Concrete covers lateral sides of configuration.

ORNL-PHOTO 3826-83

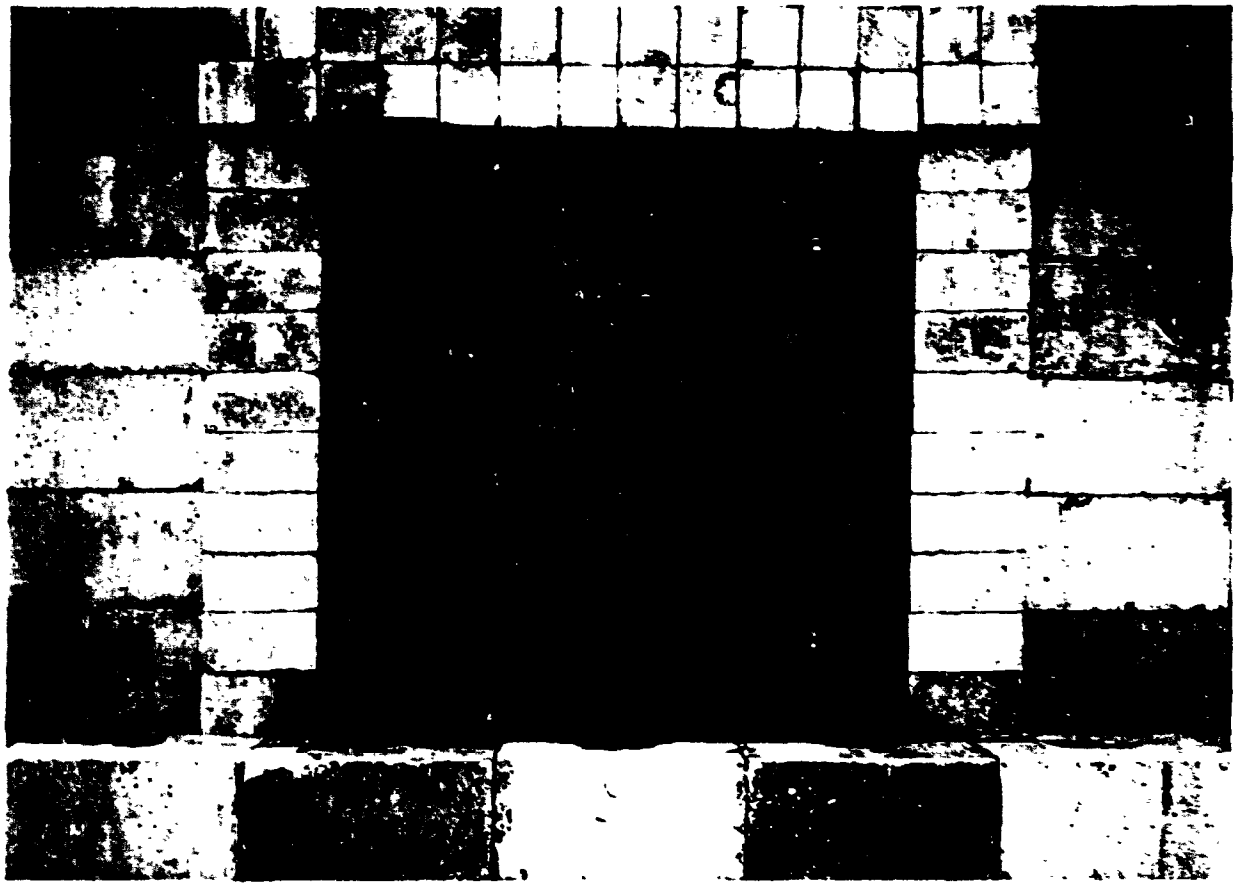

Fig. 8. Photograph of reflector layer (Items II B and III B).

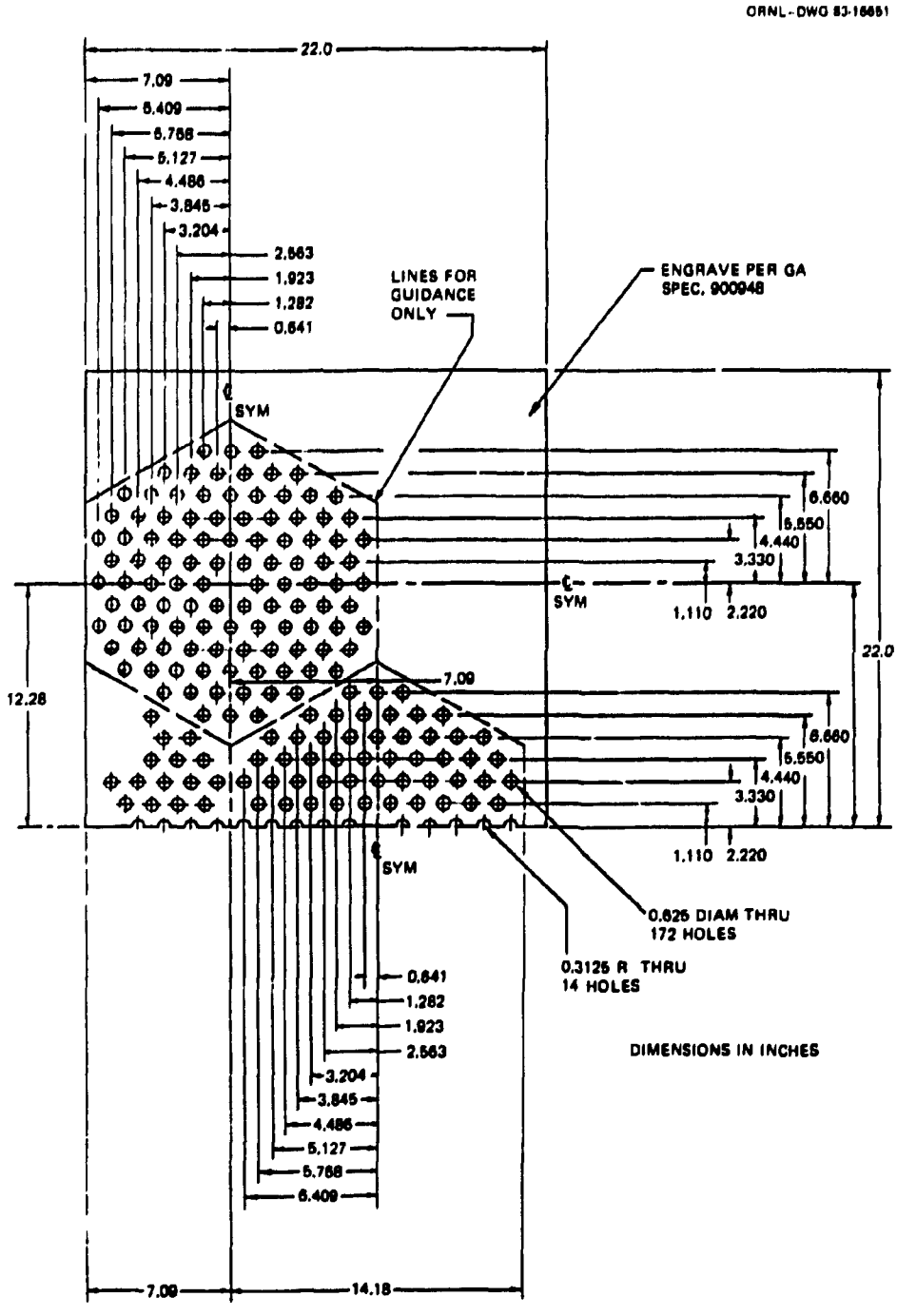

Fig. 9. Sketch of one-fourth of reflector layer (Items II B and III B).

It should be noted that in the actual HTGR design of the bottom reflector for the reactor, the small (1.588 cm diameter) coolant holes simulated in this reflector layer would be slanted to better receive coolant gas flowing upward from large coolant holes in the next layer (see Sect. 3.4 below). However, for this experimental model, the holes in the reflector layer were drilled parallel to the axis of the model.

3.4 CROSSOVER LAYER

Like the preceding layers, the crossover layer was graphite that was also assembled in four pieces. It was 40.6 cm thick (16 in.) and contained seven large coolant holes whose centerlines were coincident with the axes of the seven hexagons defined in the reflector layer. The six outer holes had diameters of 19.18 cm (7.55 in.), and the center hole had a diameter of 16.76 cm (6.60 in.). Since the small coolant holes in the reflector layer were not slanted for this experiment, some of the holes were located outside the diameter of the large hole and were abruptly ended at the reflector crossover interface. A photograph of the crossover layer as mocked up for this experiment is shown in Fig. 10.

It is also apparent from Fig. 10 that the ends of the coolant holes in the center hexagon that project from the reflector layer into the crossover layer are not directly exposed to the larger center hole that follows. Instead, the smaller coolant holes in the center hexagon are dead-ended approximately halfway through the layer as shown in Fig. 11. Again, this is a design criterion for this experiment only, for in the HTGR the holes would slant and flow into the big hole. The large center hole extending through the remainder of the layer was then connected to each of the six outer holes via 7.62-cm-diameter (3-in.) voids.

A diagram of the experimental configuration with the crossover layer added is shown in Fig. 12.

3.5 FOLLOW-ON LAYER

The last layer added to the mockup was the follow-on layer, referred to as layer D in the experimental plan in Appendix A. As were the preceding layers, the follow-on layer was made of four pieces of graphite. It was 35.8 cm thick (14.1 in.) and provided for the continuation of the six large outer coolant holes from the crossover layer. It did not, however, provide for a continuation of the center hole, which was dead-ended at the inner surface of the follow-on layer as shown in Figs. 13 and 14. The corresponding full experimental configuration is shown in Fig. 15.

3.6 CONFIGURATION DIMENSIONS: PART I vs. PART II

As mentioned earlier, the only difference in the composition of the experimental mockup for the Part I and Part II measurements was the replacement of the graphite pins in the upper pin layer in Part I with boronated graphite pins. However, to exchange the pins it was necessary to remove all four layers of the mockup, and repositioning them led to small differences in the distances from the backs of the configurations to the center of the reactor. These differences are noted in Table 8, which gives the dimensions from the reactor center to the back of each layer for both sets of measurements. Note that the dimensions given on the schematics of the various configurations referred to earlier are the dimensions for the Part I measurements.

ORNL-PHOTO 3689-83

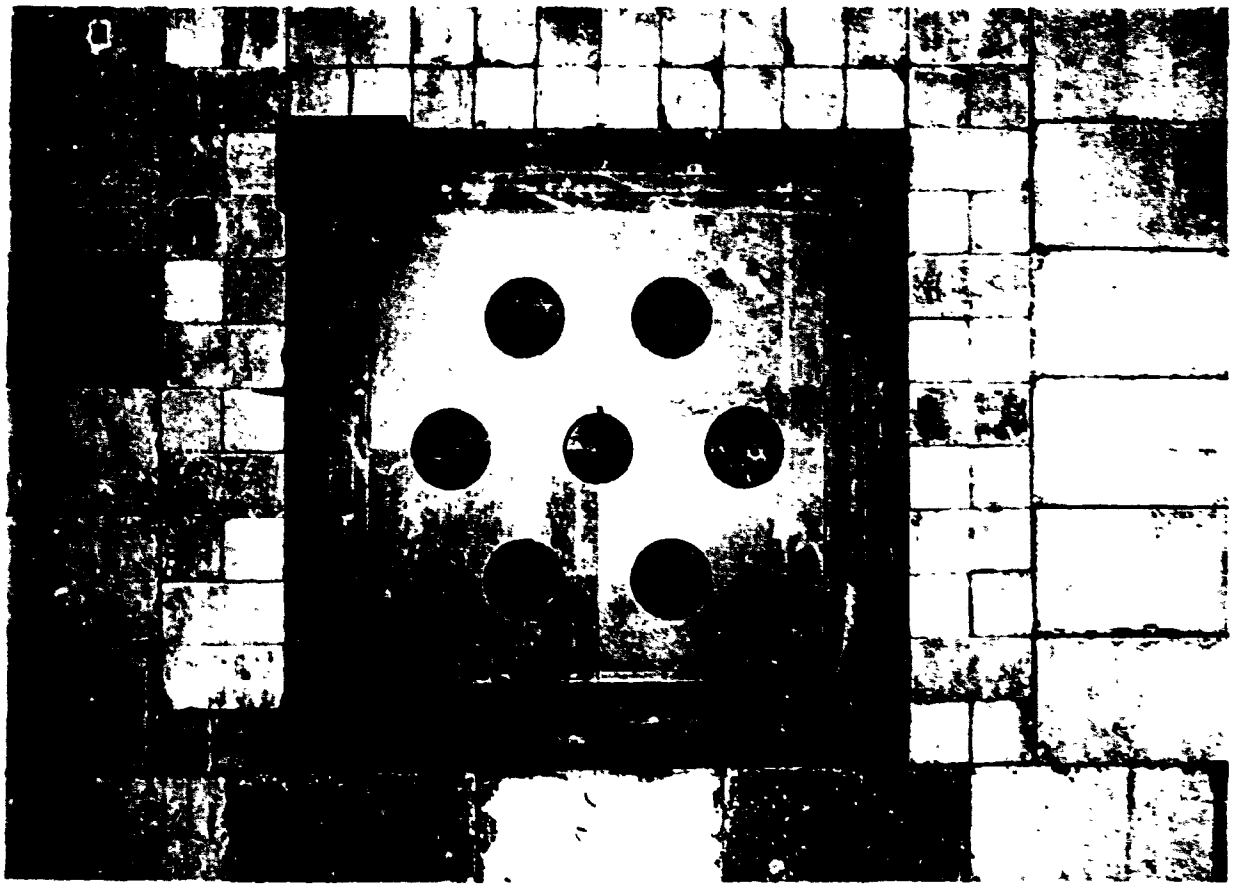

Fig. 10. Photograph of crossover layer (Items II C and III C).

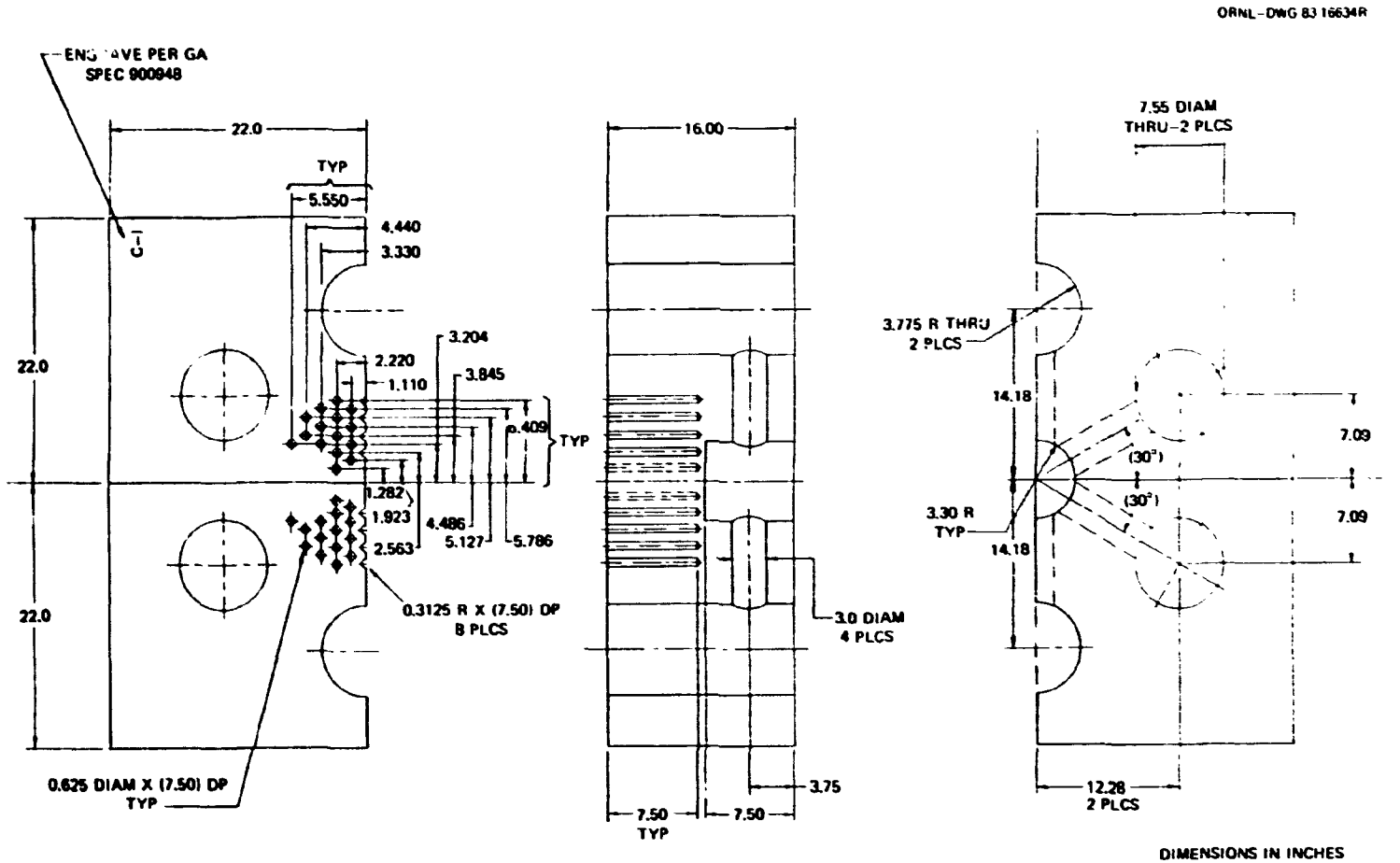

Fig. 11. Sketch of one-half of crossover layer (Items II C and III C).

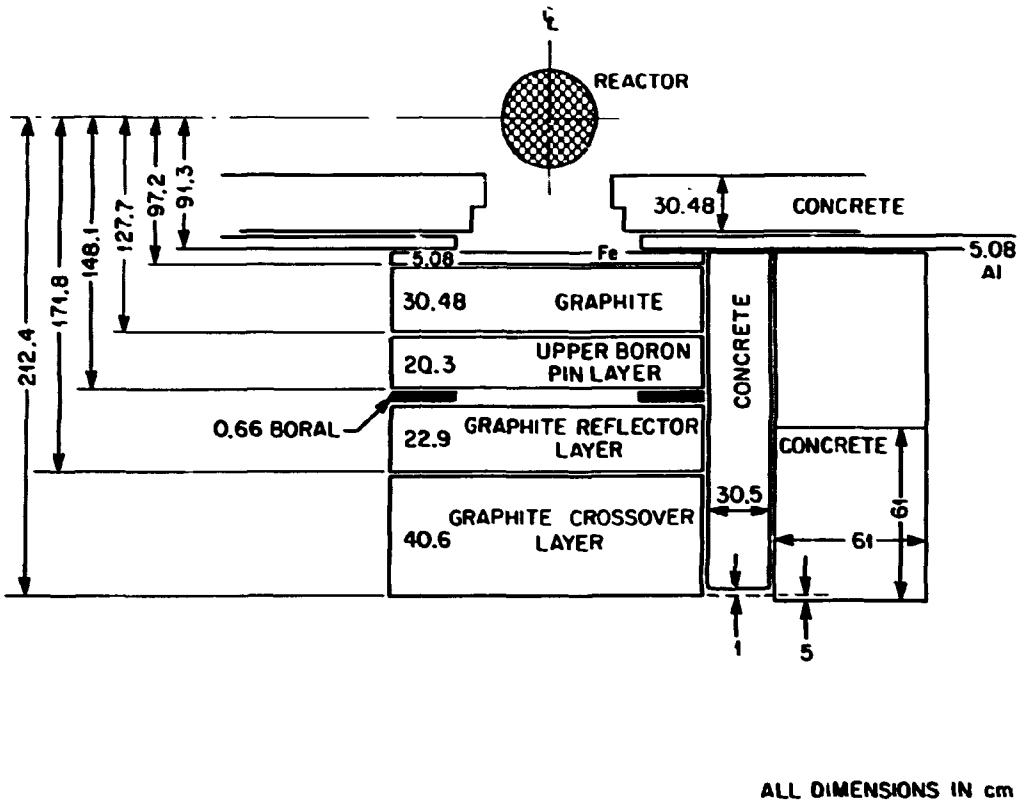

Fig. 12. Schematic of configuration containing SM + upper boron pin layer + boral shroud + reflector layer + crossover layer (Item II C). Note: Concrete covers lateral sides of configuration.

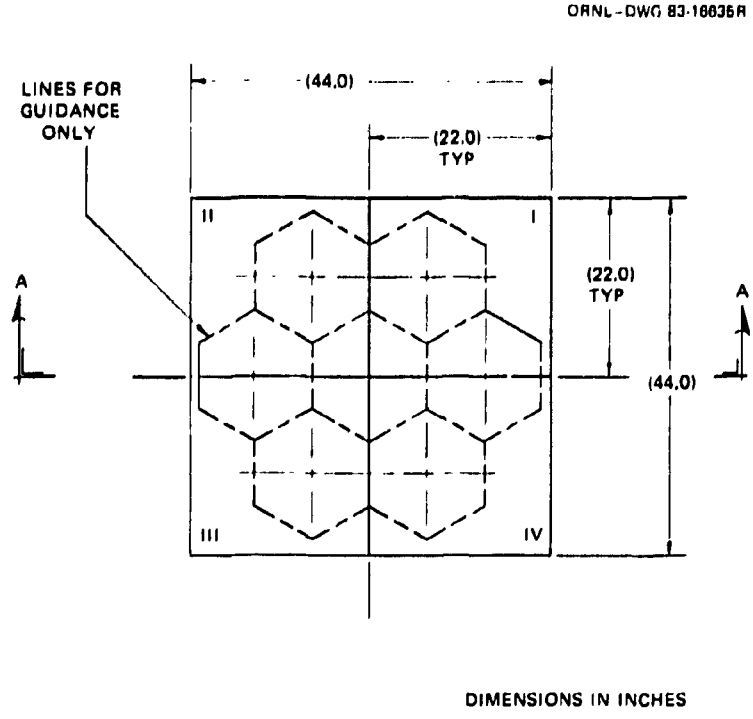

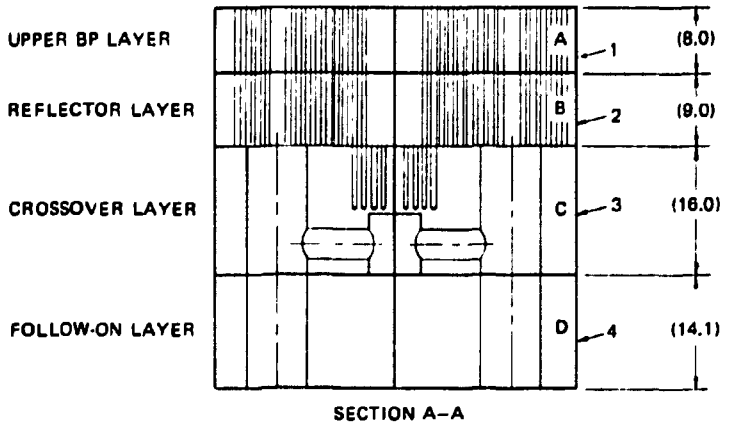

Fig. 13. Schematic of full mockup (Items II D and III D).

ORNL-PHOTO 3690-83

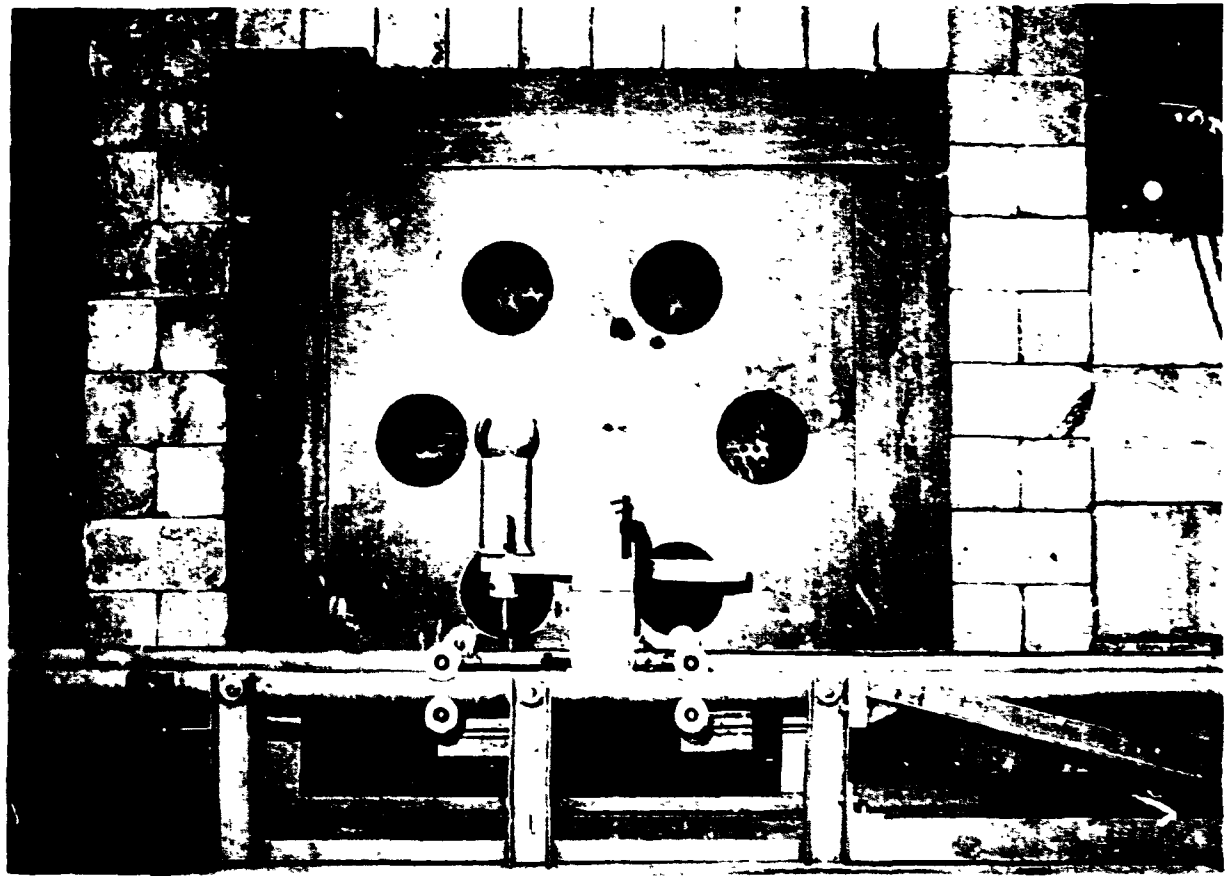

Fig. 14. Photograph of follow-on layer (Items II D and III D).

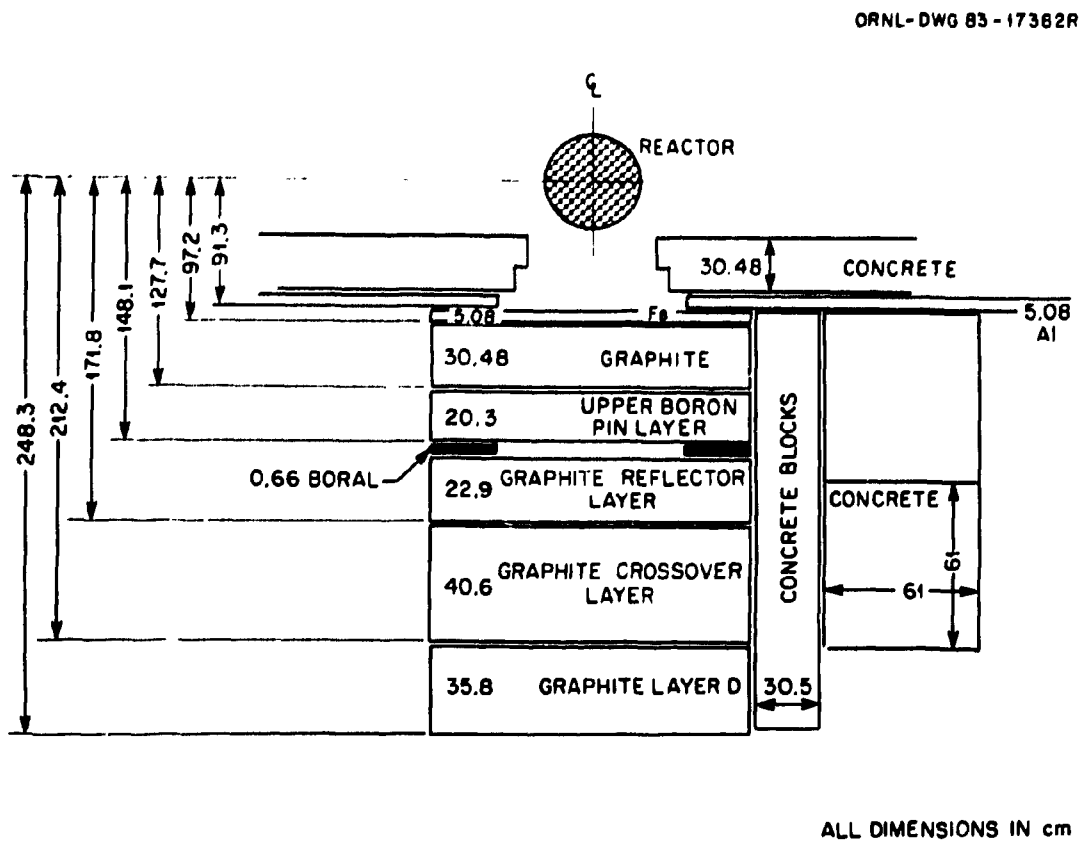

Fig. 15. Schematic of full mockup: SM + upper boron pin layer + boral shroud + reflector layer + crossover layer + follow-on layer (Item II D). Note: Concrete covers lateral sides of configuration.

4. SPECTRUM MODIFIER MEASUREMENTS (Items I A, I AA)*

Measurements of the spectra of fast neutrons behind the SM were made with both the NE213 liquid scintillator and the hydrogen-filled proton-recoil detectors. Each detector was located on the beam centerline 125.4 cm behind the graphite and was protected from high gamma-ray fluxes by the intervening 15.4-cm-thick iron slab shown in Fig. 1. The iron slab was positioned 34 cm behind the SM, which left 76 cm between the back of the slab and the detector. The resulting energy spectra are plotted in Figs. 16 and 17 and listed in Tables 9 and 10 for the NE213 spectrometer and the proton-recoil detector, respectively.

Integral neutron flux measurements with the 3-, 6-, and 10-in.-diameter Bonner balls were also made on the beam centerline 125.4 cm behind the SM, both with and without the intervening iron slab. These results are shown in the first two lines of Table 11.

* Refer to item numbers in data plan given in Appendix A.

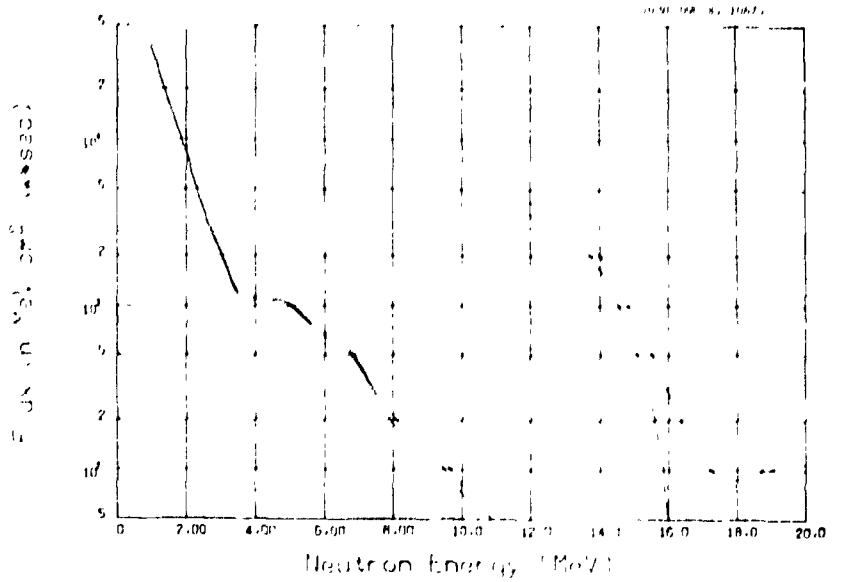

Fig. 16. Spectrum of high-energy neutrons (>0.8 MeV) on centerline 125.4 cm beyond spectrum modifier (Item I A): Run 7831A.

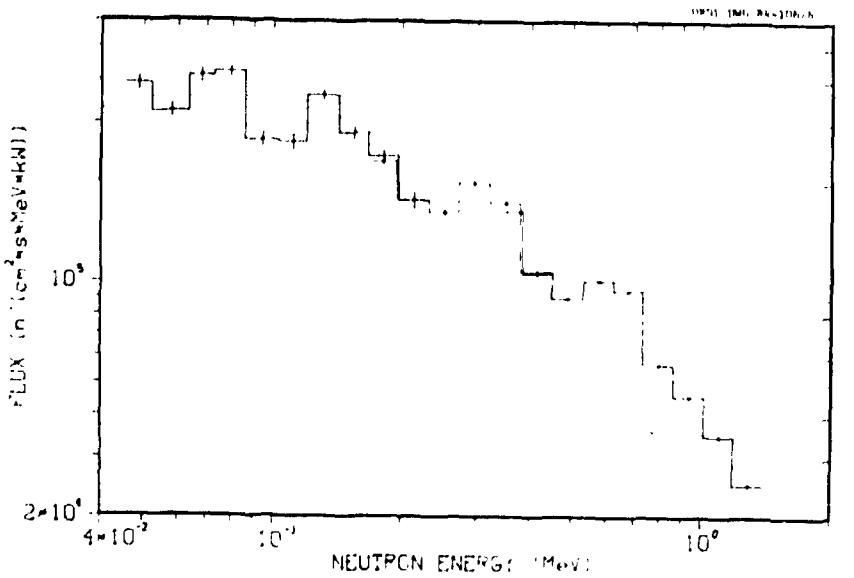

Fig. 17. Neutron spectrum (50 keV to 1.4 MeV) on centerline 125.4 cm beyond spectrum modifier (Item I A): Runs 1503A, 1502A, 1501B.

Finally, with the iron slab removed, Bonner ball traverses were made in the horizontal midplane of the configuration at two specified distances behind the SM. In one series, measurements were made with the bare BF_3 counter, the Cd-covered counter, and the 5-in.-diameter Bonner ball as close behind the SM as was feasible. In another, measurements were made with these three detectors plus the 10-in.-diameter Bonner ball at a distance of 30 cm behind the SM. The data from these traverses are presented in Tables 12 and 13, respectively.

Following the above measurements, the upper boron pin layer (with 770 BG pins and 738 graphite pins) was temporarily positioned 15 cm behind the SM and the Bonner ball measurements close behind the SM were repeated. The results of these measurements, given in Table 14, show a substantial increase in the count rate due to neutrons that were backscattered by the boron pin layer. (For these runs the boron pin layer was not surrounded by concrete.)

5. PART I MEASUREMENTS: CONFIGURATIONS WITH REFERENCE PIN PATTERN

5.1 SM + UPPER BORON PIN LAYER (Items II A, AA, AAA, AAAA)

For the measurements listed under Section II of the data plan, the reference pin pattern was used in the upper boron pin layer; that is, the layer contained 770 BG pins and 738 graphite pins at the locations indicated in Fig. 4. Neutron spectral measurements were made on the beam centerline at a distance of 134.5 cm behind the boron pin layer with both the NE213 spectrometer and the hydrogen-filled proton-recoil counters. Again it was necessary to insert the 15.4-cm-thickness of iron between the mockup and the spectrometers to reduce the gamma-ray intensity at the detector location. The resulting spectra are plotted in Figs. 18 and 19 and listed in Tables 15 and 16 for the NE213 spectrometer and the proton-recoil counter, respectively.

Integral neutron flux measurements were also made at the 134.5-cm distance with the 3-, 6-, and 10-in.-diameter Bonner balls, both with and without the intervening iron slab, and the results are included in Table 11.

Bonner ball measurements were made beyond the boron pin layer along traverses in both the vertical midplane and the horizontal midplane of the experimental configuration. The results from a vertical traverse with the 5-in.-diameter ball at a distance of 30 cm behind the mockup are given in Table 17, and those from horizontal traverses with the bare and Cd-covered counters as close as feasible behind the configuration are given in Table 18. The results of a horizontal traverse with the bare and Cd-covered BF_3 counters and the 5- and 10-in.-diameter Bonner balls at a distance of 30 cm are given in Table 19, and measurements with the same detectors on the beam centerline at a distance of 300 cm beyond the configuration are given in Table 20. (An attempt was made to also perform Hornyak button measurements directly behind the configuration to define possible neutron-streaming effects down the coolant holes, but the idea was abandoned when it was noticed that the gamma-ray flux was so strong compared to the fast-neutron flux that obtaining meaningful data would not be possible.)

As called for under Item II AA in the data plan, horizontal traverses with the bare and Cd-covered BF_3 counters were also made close behind the boral shroud following the boron pin layer. These data are compared with those taken directly behind the boron pin layer in Table 18.

For the final series of measurements behind the boron pin layer, the reflector layer was temporarily positioned 15 cm behind the boron pin layer, and measurements were made with the bare and Cd-covered BF_3 counters along a horizontal traverse in the intervening gap, both with and without the boral shroud present. The results are given in Table 21.

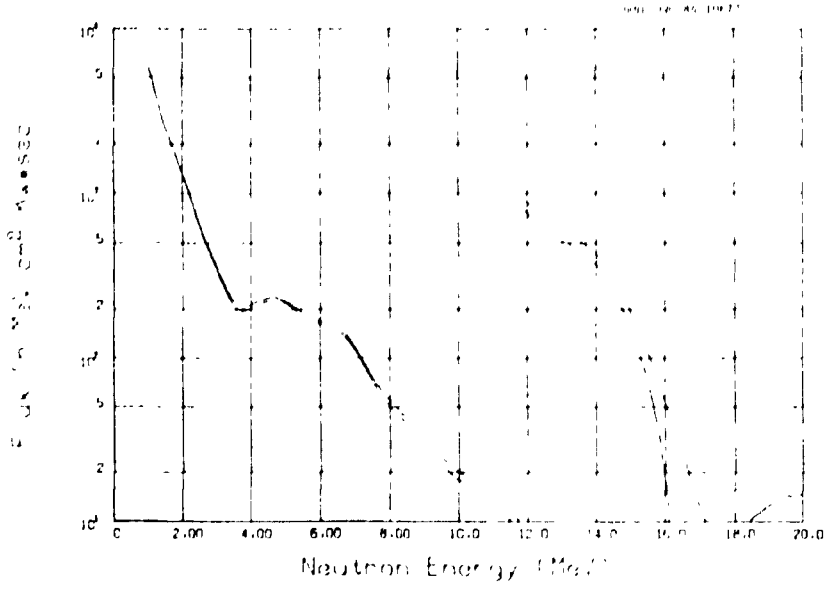

Fig. 18. Spectrum of high-energy neutrons (>0.8 MeV) on centerline 134.5 cm beyond upper boron pin layer (Item II A, reference pin pattern): Run 7833B.

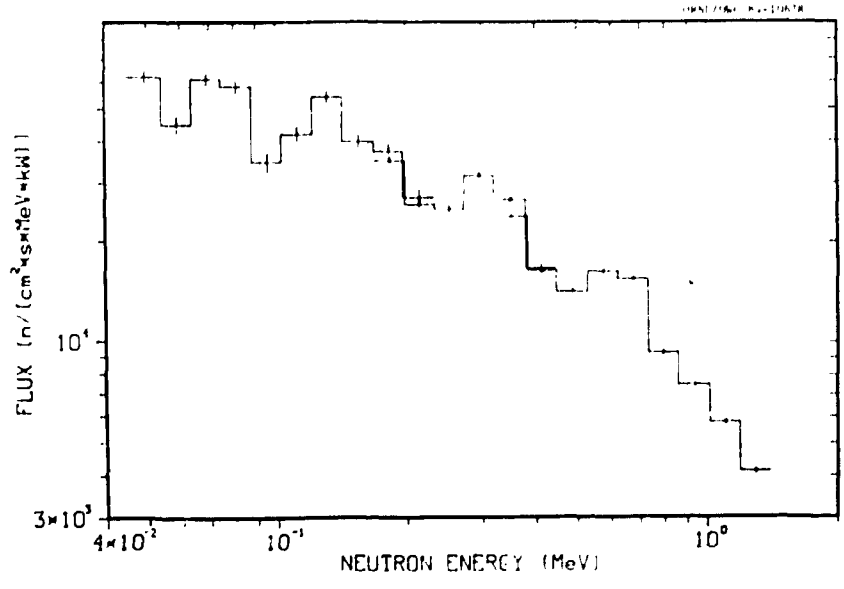

Fig. 19. Neutron spectrum (50 keV to 1.4 MeV) on centerline 134.5 cm beyond upper boron pin layer (Item II A, reference pin pattern): Runs 1506A, 1508C, and 1505A.

5.2 SM + UPPER BORON PIN LAYER + BORAL SHROUD + REFLECTOR LAYER (Items II B, BB)

After the reflector layer was added to the mockup, only Bonner ball measurements were made. (The intensities of the high-energy neutrons beyond the reflector layer and the subsequent layers had been sufficiently reduced to preclude making meaningful spectral measurements.)

The first measurements behind the reflector layer were traverses in the horizontal midplane of the configuration with the bare and Cd-covered counters as close behind the configuration as was feasible (see Table 22). Horizontal traverses were also made with the bare and Cd-covered counters and with the 5- and 10-in.-diameter Bonner balls at a distance of 30 cm beyond the configuration (see Table 23). In addition, measurements were made with all four detectors on the beam centerline at a distance of 300 cm beyond the configuration (see Table 20).

Again, the next layer of the mockup — in this case, the crossover layer — was placed 15 cm behind the configuration, and measurements were made with the bare and Cd-covered counters along horizontal traverses within the void. These count rates are given in Table 24.

5.3 SM + UPPER BORON PIN LAYER + BORAL SHROUD + REFLECTOR LAYER + CROSSOVER LAYER (Items II C, CC)

The same series of measurements described in Sect. 5.2 were repeated behind the configuration in which the crossover layer had been added. Data from the traverses close behind the configuration are included in Table 22, those from the traverses 30 cm beyond the configuration are given in Table 25, and those obtained on the beam centerline 300 cm beyond the configuration are included in Table 20. The data obtained within the void formed by the addition of the follow-on layer 15 cm behind the crossover layer are included in Table 24.

5.4 SM + UPPER BORON PIN LAYER + BORAL SHROUD + REFLECTOR LAYER + CROSSOVER LAYER + FOLLOW-ON LAYER (Item II D)

The addition of the follow-on layer (layer D) beyond the crossover layer completed the experimental mockup for the Part 1 measurements. Again, measurements were made close behind the mockup (see Table 22), 30 cm beyond the mockup (see Table 26), and on the beam centerline 300 cm beyond the mockup (see Table 20).

In addition to the above, measurements were made with the bare and Cd-covered counters along the axis of the large coolant hole that was located directly to the left of the center hexagon as one looks from behind the configuration toward the reactor. The traverses began near the reflector segment, passed through both the crossover layer and the follow-on layer and then continued beyond the configuration for several centimeters. Data for these measurements are given in Table 27.

6. PART II MEASUREMENTS: CONFIGURATIONS WITH FULL PIN PATTERN

6.1 SM + UPPER BORON PIN LAYER (Items III A, AA, AAA, AAAA)

For this part of the experiment the number of BG pins in the upper pin layer was increased from 770 to 1508 by replacing all of the graphite pins in the reference pin pattern with BG pins (except the four permanent graphite pins described in Sect. 3.1). As noted earlier, this pin pattern is referred to as the full pin pattern. The measurements behind the boron pin layer with this pattern were compared with those behind the layer with the reference pin pattern to show the effect that the additional boron in the layer had on neutrons streaming through the support block.

Neutron spectra were obtained with both the NE213 spectrometer and the hydrogen-filled proton-recoil detectors on the beam centerline at a distance of 125.5 cm behind the boron pin layer, and, again, the spectrometers were protected from the high gamma-ray flux by the 15.4-cm thickness of iron. The spectral data for the NE213 spectrometer and the hydrogen counters are plotted in Figs. 20 and 21, respectively, and are listed in Tables 28 and 29, respectively. Bonner ball data obtained at the same location, with and without the iron present, are included in Table 11.

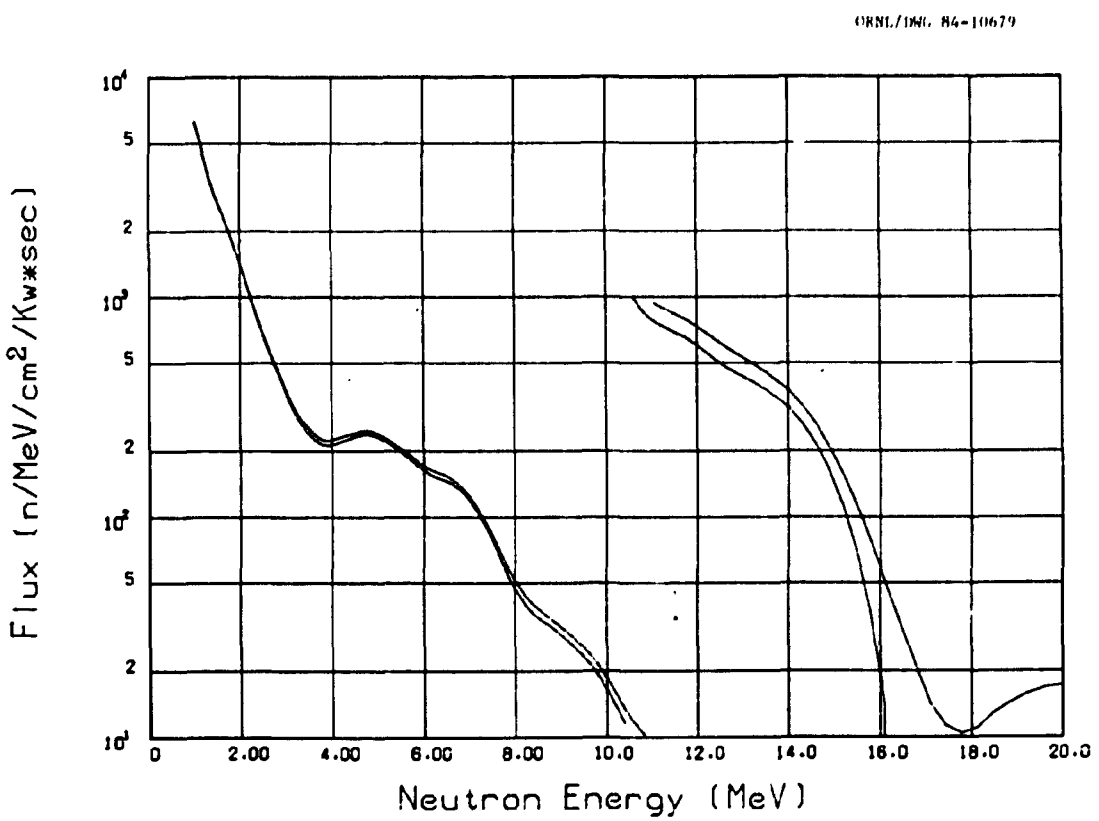

Fig. 20. Spectrum of high-energy neutrons (>0.8 MeV) on centerline 125.5 cm beyond upper pin layer (Item III A, full pin pattern): Run 7835B.

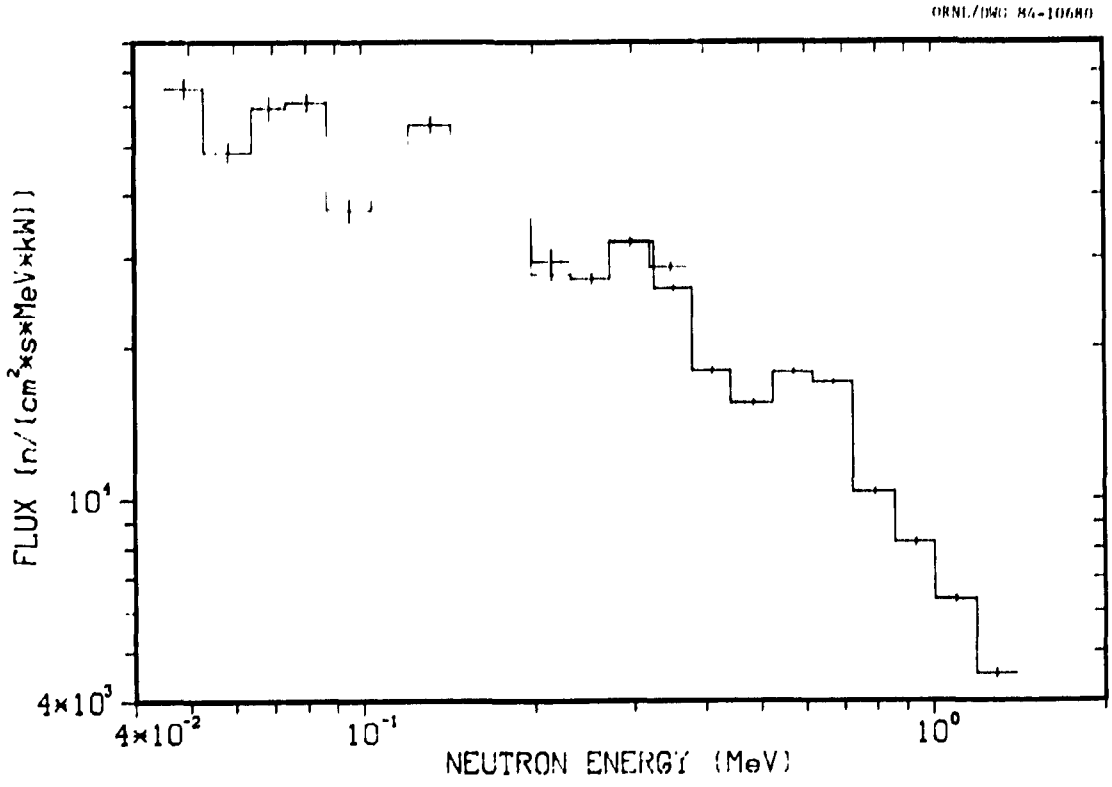

Fig. 21. Neutron spectrum (50 keV to 1.4 MeV) on centerline 125.5 cm beyond upper boron pin layer (Item III A, full pin pattern): Runs 1511A, 1510A, and 1509B.

Bonner ball measurements were also made beyond the configuration along traverses in both the vertical midplane and the horizontal midplane of the configuration. The results of a vertical traverse with the 5-in.-diameter ball 30 cm beyond the configuration are included in Table 17 and those from horizontal traverses with the bare and Cd-covered counters and with the 5- and 10-in.-diameter balls, also 30 cm beyond the configuration, are presented in Table 30. Data obtained with these same detectors on the centerline 300 cm behind the configuration are included in Table 20.

Measurements with the bare and Cd-covered counters were also made close behind the mockup, both with and without the boral shroud behind the upper pin layer (see Table 31). Finally, the reflector layer was placed 15 cm beyond the upper pin layer, and the measurements were repeated in the void between the pin layer and the reflector layer, both with and without the boral shroud present. These data are given in Table 32.

6.2 SM + UPPER BORON PIN LAYER + BORAL SHROUD + REFLECTOR LAYER (Items III B, BB)

The measurements behind this configuration were essentially repeats of those described in Sect. 5.2. The results from horizontal traverses close behind the reflector layer with the bare and Cd-covered

counters are given in Table 33, and those from horizontal traverses 30 cm beyond the configuration with the bare and Cd-covered counters and the 5- and 10-in.-diameter Bonner balls are given in Table 34. The centerline measurements 300 cm behind the reflector layer with these same four detectors are included in Table 20. And the data from the horizontal traverses with the bare and Cd-covered counters within the 15-cm-thick void between the reflector and crossover layer are given in Table 35.

6.3 SM + UPPER BORON PIN LAYER + BORAL SHROUD + REFLECTOR LAYER + CROSSOVER LAYER (Items III C, CC)

As was the case for the two previous layers, these measurements in Part II beyond the crossover layer were repeats of those made behind the crossover layer in Part I (see Sect. 5.3). The results from the horizontal traverses close behind the crossover layer with the bare and Cd-covered counters are included in Table 33, and those from the horizontal traverses 30 cm beyond the crossover layer with the bare and Cd-covered counters and the 5- and 10-in.-diameter Bonner balls are given in Table 36. Data obtained from the horizontal traverses with the bare and Cd-covered counters within the void created when the follow-on layer was positioned 15 cm behind the crossover layer are included in Table 35. Results from the measurements with the four detectors on centerline at the 300-cm point are included in Table 20.

6.4 SM + UPPER BORON PIN LAYER + BORAL SHROUD + REFLECTOR LAYER + CROSSOVER LAYER + FOLLOW-ON LAYER (Item III D)

For this final experimental configuration, horizontal traverses were again made as close behind the mockup as possible with the bare and Cd-covered counters (see Table 33), at a distance of 30 cm beyond the configuration with the bare and Cd-covered counters and the 5- and 10-in.-diameter Bonner balls (see Table 37), and on the beam centerline at the 300-cm distance with all four detectors (see Table 20). Finally, measurements were made again along the axis of the same large coolant hole described in Sect. 5.4. These results are given in Table 38.

7. ANALYSIS OF EXPERIMENTAL ERRORS

The errors associated with the measurements are due to a number of uncertainties: in the sizes of voids unavoidably introduced in the configurations; in the positions of the detectors and in their count rate statistics and calibrations; in the reactor power determinations; and in the effects of the exposure of the configurations to the weather. Of these, the uncertainty due to exposure is the least understood and probably beyond simple estimation. The uncertainty is associated with the moisture absorbed within the graphite and the concrete placed around the graphite and its effect on the neutron transmission through the mockup. During the experiment, however, the configurations were covered with a tarpoulin to minimize this effect. Best estimates would put the variation in attenuation for the low-energy neutrons under 10%, with even less change occurring for the high-energy neutrons.

In order to minimize the void spacings between segments in the configurations, the graphite pieces used in the mockup were precisely machined and had smooth, flat surfaces that allowed relatively accurate positioning. Thus the error in determining the thickness of the mockups in this experiment was small.

Movement of the Bonner balls along a traversing mechanism can vary the detector location with respect to the configuration several millimeters on either side of a straight line. For the measurements close behind the configurations (at a distance of approximately 4 cm), such variations in the detector position could amount to a change in the count rate of about 5%. For the measurements 30 cm beyond the configurations, the change would probably be less than 1 to 2%.

The errors attributed to the measurements are expressed in a manner appropriate to each detector system. For the NE213 spectrometer, only the counting statistics and unfolding errors are included in the unscrambling of the pulse-height spectra with the FERD code, with the resultant flux being expressed in terms of lower and upper limits that represent a 68% confidence level. Similar errors are calculated for the hydrogen counter measurements unfolded with SPEC 4. For the Bonner balls, the statistical error in the detector count rate was kept to 1 to 2% by collecting an adequate number of counts. Calibrations of the detector over the experimental period indicated less than a 5% spread.

The TSR-II power level for each measurement was determined from the output of two fission chambers located in the reactor shield along the midplane of the reactor. The response of these chambers to the reactor source was monitored prior to the experiment through the use of gold foils and found to agree, within several percent, to the established reactor power values. These detectors were calibrated on a daily basis using a ^{252}Cf source, with the calibration values lying within about a 6% spread ($\pm 3\%$ of an average value). During any one detector traverse in a given day, the variation in the reactor power indicated by the monitor outputs was at most only a few percent; however, during the several months the experiment was being performed, the monitors indicated variations of about $\pm 5\%$. Thus, the uncertainty in the reactor power determination was assumed to be $\pm 5\%$.

Rather than calculate probable errors for each one of a series of measurements in a traverse or for any one traverse, we prefer, in general, to quote a value for the error in the measurements for a given experiment. Thus, assuming the estimated upper limit for all the errors, the errors assigned to the Bonner ball measurements should be less than $\pm 10\%$. For the spectral measurements, it should be noted that they do not reflect the uncertainties associated with the reactor power determination, which could be, as discussed above, as high as 5%.

8. DISCUSSION OF RESULTS

8.1 SPECTRAL MEASUREMENTS

The measurements of the energy spectra of neutrons behind the spectrum modifier (see Figs. 16 and 17) and behind the two boron pin layers, one containing the reference pin pattern (Figs. 18 and 19) and the other the full pin pattern (Figs. 20 and 21), showed that the spectra of fast neutrons behind the boron pin layers were essentially the same both in magnitude and in shape, and, further, that the spectrum observed behind the spectrum modifier also had the same shape. Both boron pin layers reduced the magnitude of the spectrum by about a factor of five.

8.2 BONNER BALL MEASUREMENTS

Bare Counter Measurements 30 cm Beyond Configurations. The count rates from the horizontal traverses with the bare BF_3 counter at a distance of 30 cm beyond the various configurations for both pin patterns are compared in Fig. 22. The figure shows that the count rates behind the boron pin layers

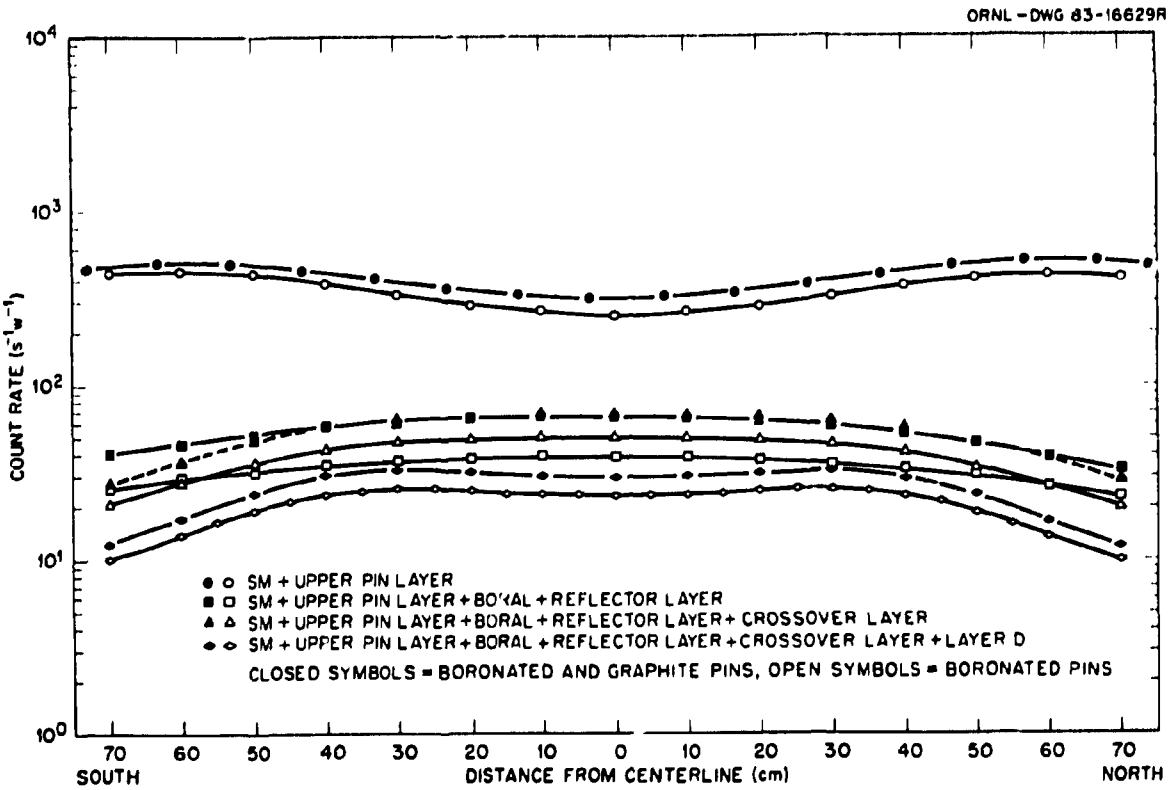

Fig. 22. Count-rate profiles for bare BF_3 counter along horizontal traverses 30 cm beyond each configuration (Items II A-D and III A-D).

were somewhat lower in the vicinity of the centerline than near the edges of the configurations for both the reference pin pattern and the full pin pattern. The figure also shows that replacing the graphite pins in the reference pin pattern with BG pins reduced the count rates by about 20%.

With the boral shroud and the reflector layer added to the configurations, the difference between the bare counter curves for the two pin patterns is more pronounced and the shapes of the curves are altered. The count rates on the centerline behind the configurations were reduced by a factor of four for the reference pin pattern and by a factor of six for the full pin pattern. Near the edges of the configuration the reduction was greater due to the presence of the boral outside the pin area between the upper pin layer and the reflector, but the spread between the curves for the two pin patterns was less.

When the crossover layer was added to the configuration containing the reference pin pattern, the count rate from the bare counter was unchanged (within the hexagon areas only) from that observed behind the reflector layer. Beyond the pin area there was a noticable decrease. However, adding the crossover layer to the configuration containing the full pin pattern *increased* the count rate on the centerline by 30%. Beyond the pin area the count rates fell below those at corresponding positions behind the reflector layer.

The addition of the follow-on layer (layer D) to the configurations decreased the count rates by a factor of about two for both pin patterns. Again, the shapes of the curves were altered, this time reflecting the higher neutron streaming through the large outer coolant holes.

Cd-Covered Counter Measurements 30 cm Beyond Configurations. The count rates for the horizontal traverses with the Cd-covered BF_3 counter at a distance of 30 cm beyond the various configurations for both pin patterns are compared in Fig. 23. As was the case for the measurements with the bare counter, the count rates obtained with the Cd-covered counter behind the boron pin layer reflect a depression in the neutron flux in the vicinity of the centerline, especially for the full pin pattern. Comparing the count rates obtained behind the two boron pin layers with the bare and Cd-covered counters (compare Figs. 22 and 23) shows that the count rates obtained with the Cd-covered counter were a factor of 20 lower than those obtained with the bare counter for the reference pin pattern and nearly a factor of 30 lower for the full pin pattern.

As was observed for the bare counter in Fig. 22, adding the boral shroud and reflector layer to the configuration altered the shapes of the count rate curves for the Cd-covered counter. The count rates for both pin arrangements were reduced by a factor of about two on the centerlines and a factor of about four near the edges, so that the depression in the centerline fluxes observed in the measurements behind the boron pin layer disappeared.

For both pin patterns, the count rates for the Cd-covered counter were decreased when the crossover layer was added to the configurations; however, the curves for the two configurations differ in magnitude by only about 20%. Both curves give some indication of neutron streaming from the outer coolant holes.

When the follow-on layer (layer D) was added, further reductions in the count rates from the Cd-covered counter were observed, and the streaming through the outer coolant holes was accentuated. Figure 23 shows that while the count rates on the centerline were reduced by a factor of five for both pin patterns, the count rates behind the coolant holes were reduced only a factor of three.

Comparing Figs. 22 and 23 indicates that, overall, as the layers were added to the configurations, the differences between the count rates obtained with the Cd-covered counter for the two pin patterns are less than those obtained with the bare counter in corresponding measurements.

5-in.-diameter Bonner Ball Measurements 30 cm Beyond Configurations. The results of the horizontal traverses 30 cm beyond the configurations with the 5-in.-diameter Bonner ball are presented in Fig. 24. These curves are very similar in shape to those given in Fig. 23 except that (1) no depression of the flux in the vicinity of the centerline is observed until the crossover layer is added and (2) neutron streaming through the outer coolant holes is slightly more pronounced. Again, the differences in the count rates for the two pin patterns decreased as layers were added to the configurations.

10-in.-diameter Bonner Ball Measurements 30 cm Beyond Configurations. The count rates observed with the 10-in.-diameter Bonner ball 30 cm beyond the configurations are plotted in Fig. 25. The shapes of the curves are essentially the same as those for the 5-in. ball, but the magnitudes are lower by a factor of about three. The effect of the additional BG pins in the full pin pattern is much less pronounced for this ball, the differences in the two pin patterns decreasing to essentially zero behind the follow-on layer (layer D).

Bare Counter Measurements Close Behind Configurations. The data obtained from horizontal traverses with the bare counter close behind the configurations (within 4 to 5 cm) are plotted in Fig. 26. As was the case for the bare counter data at 30 cm, the centerline measurements behind the boron pin layer with the full pin pattern were lower than those behind the layer with the reference pin pattern, and the difference increased when the boral shroud and reflector layer were added to both configurations.

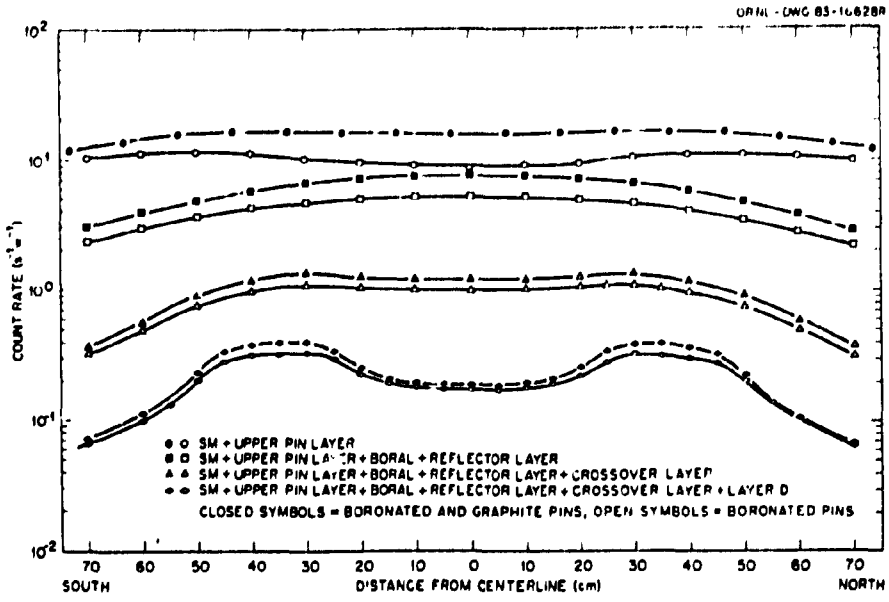

Fig. 23. Count-rate profiles for Cd-covered BF_3 counter along horizontal traverses 30 cm beyond each configuration (Items II A-D and III A-D).

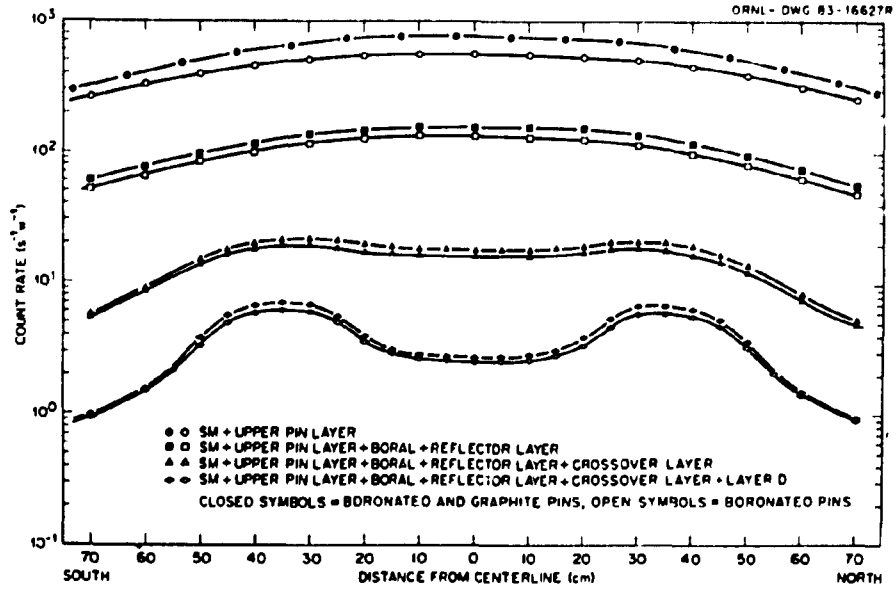

Fig. 24. Count-rate profiles for 5-in.-diameter Bonner ball along horizontal traverses 30 cm beyond each configuration (Items II A-D and III A-D).

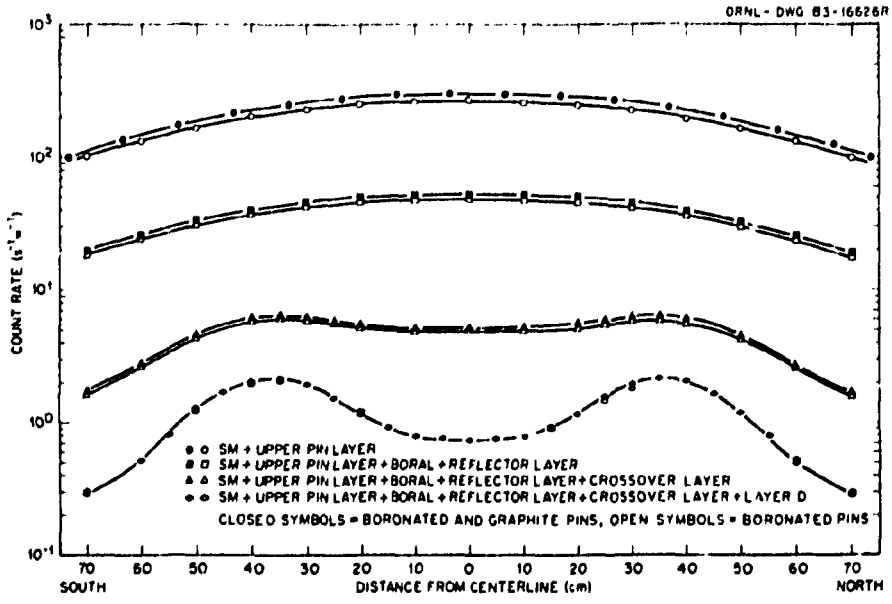

Fig. 25. Count-rate profiles for 10-in.-diameter Bonner ball along horizontal traverses 30 cm beyond each configuration (Items II A-D and III A-D).

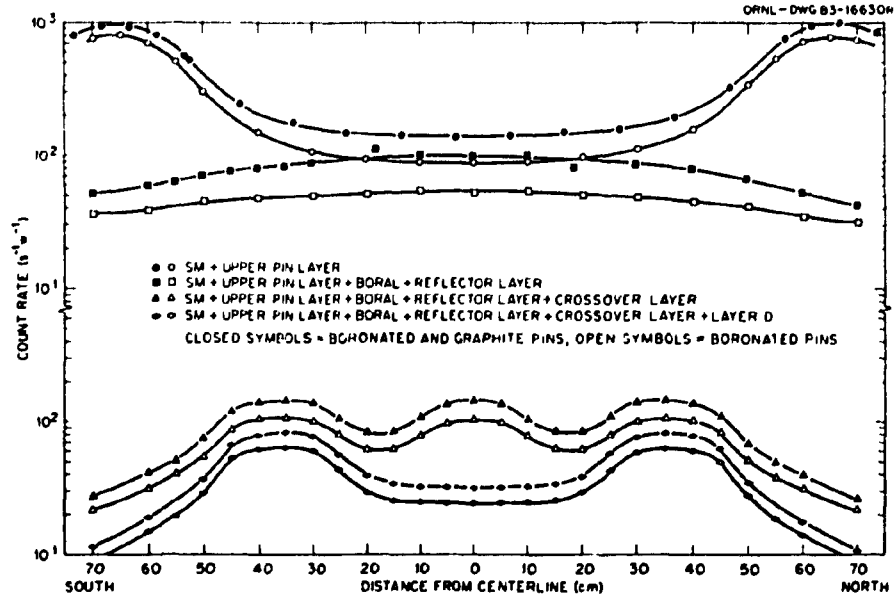

Fig. 26. Count-rate profiles for bare BF_3 counter along horizontal traverses close behind each configuration (Items II A-D and III A-D).

The bare counter measurements close behind the boron pin layer also showed that neutrons streamed through the graphite surrounding the boron pin region — to the extent that the count rates near the edges of the configurations were higher by almost a factor of 10 than those on the centerline. This streaming was reduced by a factor of 20 when the boral shroud and reflector were added behind the boron pin layer.

Once again, as occurred in the measurements at 30 cm, the addition of the crossover layer to the configurations caused a definite increase in the bare counter measurements for the full pin pattern and a slight increase in those for the reference pin pattern. In this case, the effect of streaming through the large center coolant hole and the two adjacent outer coolant holes became apparent with the addition of the crossover layer. (As noted in Fig. 22, the streaming effect was not reflected in the bare counter measurements at 30 cm.)

Neutron streaming through the outer coolant holes is also apparent in the bare counter measurements close behind the follow-on layer (layer D). The center peak has disappeared because the center coolant hole did not extend through this layer. The centerline measurements behind the follow-on layer were lower than those behind the crossover layer by a factor of about three.

Cd-Covered Counter Measurements Close Behind Configurations. Count rates from the Cd-covered counter traverses close behind the configurations are plotted in Fig. 27. The count rates behind the boron pin layer again reflect the streaming of neutrons through the graphite surrounding the pin region, but in this case the count rates in the peaks at the edges of the configurations are only slightly higher than those on the centerline.

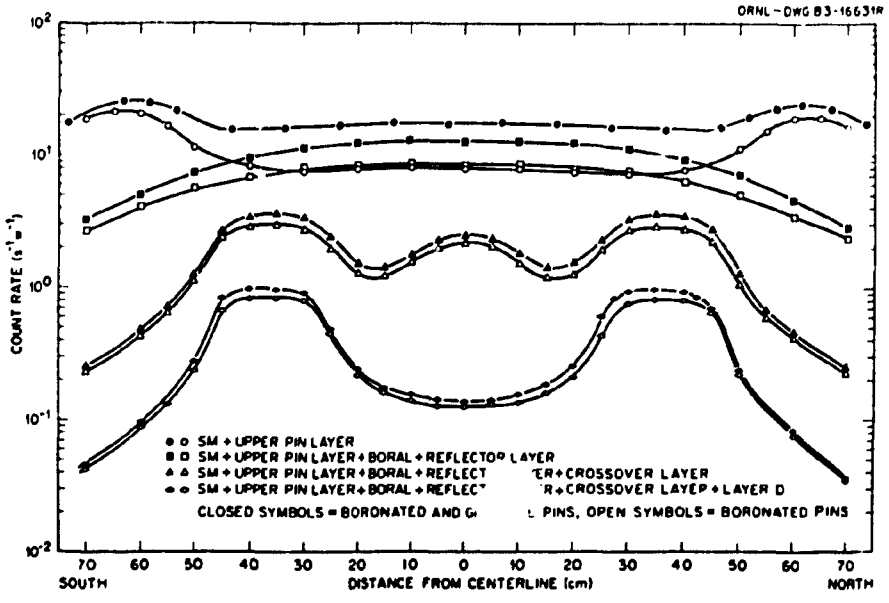

Fig. 27. Count-rate profiles for Cd-covered BF_3 along horizontal traverses close behind each configuration (Items II A-D and III A-D).

For the configuration with the full pin pattern, the addition of the boral shroud and the reflector layer did not reduce the count rates in the vicinity of the centerline (immediately behind the pin region), but the neutrons streaming at the edges of the configuration were effectively reduced. For the configuration with the reference pin pattern, the addition of the boral shroud and the reflector layer reduced the centerline fluxes somewhat and again effectively reduced the neutron streaming at the edges of the configuration.

As was the case for the measurements at 30 cm, the measurements close behind the configurations with the Cd-covered counter showed that the addition of the crossover layer similarly reduced the count rates and the differences in the measurements for the two pin patterns were again slight. However, as would be expected, the streaming effects were much more pronounced in the measurements close behind the configurations than they were at 30 cm. At the locations of the streaming peaks, the magnitudes of the count rates observed with the Cd-covered counter were lower than those observed with the bare counter by a factor of about 50.

With the addition of the follow-on layer (layer D), the peak count rates observed with the Cd-covered counter at the outer coolant hole dropped another factor of three for both pin patterns. The centerline count rates behind the closed-off center coolant holes dropped a factor of about 20, which is considerably more than the factor of five reduction observed with the bare counter. Again, the difference in the measurements with the Cd-covered counter for the two pin patterns was slight.

Bare and Cd-Covered Counter Measurements Close Behind Boron Pin Layer With and Without Boral Shroud. The effect of the boral shroud in reducing the streaming of low-energy neutrons around the boron pin region can be seen in Fig. 28, which compares measurements made close behind the boron pin layer with and without the boral shroud present.

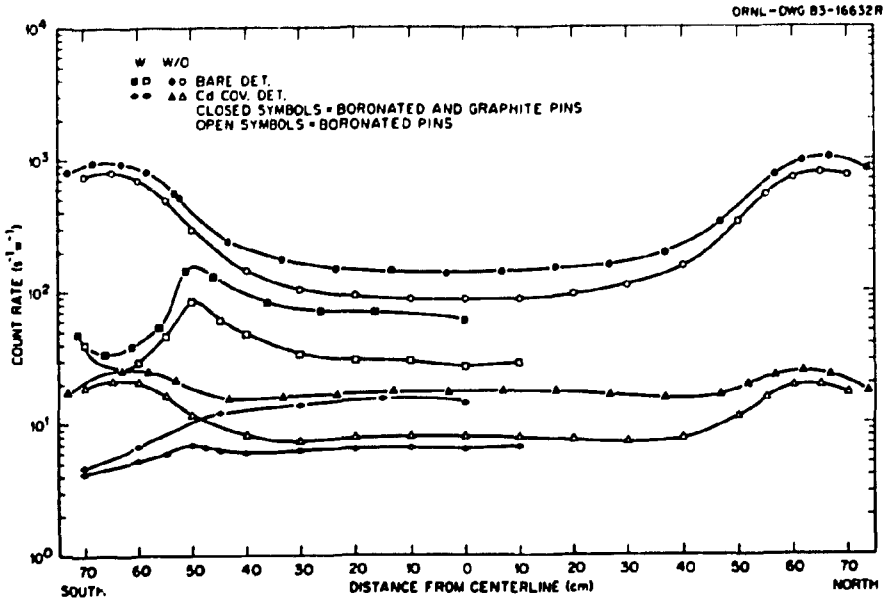

Fig. 28. Count-rate profiles for bare and Cd-covered BF_3 counters along horizontal traverses close behind boron pin layer with and without boral shroud (Items II A, AA and Items III A, AA).

For the bare counter, the boral shroud reduced the count rates directly behind the shroud itself (toward the edges of the configurations) by a factor of about 30 for both pin patterns. Not only that, it also accounted for a 50% reduction in the centerline count rate behind the boron pin layer with the reference pin pattern. With the full pin pattern in the layer, adding the boral shroud effected nearly another 50% reduction in the centerline flux, but there was little added reduction in the fluxes directly behind the boral.

For the Cd-covered counter, Fig. 28 shows that for both pin patterns the boral shroud caused a factor of four reduction in the count rates near the edges of the configurations and decreased the fluxes on the centerline by only about 10%. Again, replacing the reference pin pattern with the full pin pattern reduced the centerline fluxes by about 50%.

Bare and Cd-Covered Measurements Along Axis of Outer Coolant Hole. Measurements with the bare and Cd-covered counters along the axis of one of the large outer coolant holes are plotted in Fig. 29. The results show that the additional number of BG pins in the full pin pattern reduced the count rates of the bare counter by about 30% and those of the Cd-covered counter by about 15%.

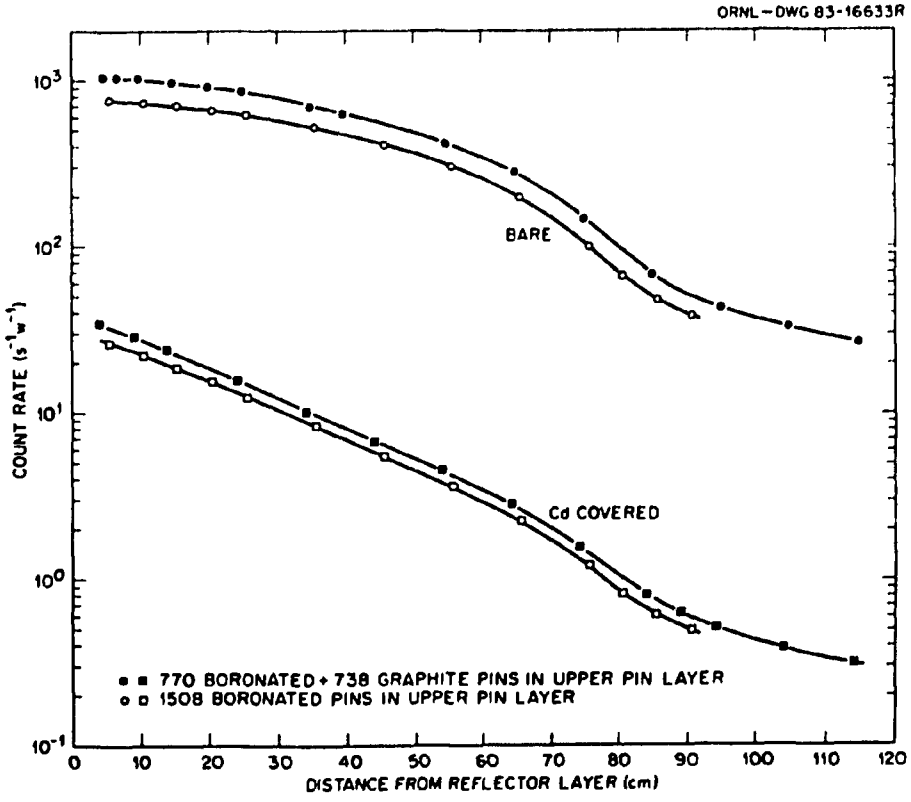

Fig. 29. Count-rate profiles for bare and Cd-covered BF_3 counters along axis of large outer coolant hole (Items II D and III D).

9. CONCLUSIONS

Experimental results indicate that there is very little difference in neutron attenuation through the first four segments of the HTGR lower reflector and core support mockup when the reference pin pattern (770 boronated graphite and 738 graphite pins) in the upper pin layer is replaced by the full pin pattern (1508 boronated graphite pins). The 10-in. Bonner ball results are essentially the same for both pin patterns behind the extension (layer D) of the crossover segments. For the 5-in. Bonner ball measurements, the count rates behind the pin mockup with the full pin pattern are about 10% lower than those behind the mockup with the reference pin pattern. The increase in the number of boron pins has the most effect in the low-energy neutron region where the bare and Cd-covered detector count rates behind the mockup with the reference pin pattern are about 25% higher than those behind the mockup with thefull pin pattern.

The attenuation through the four segments was greatest for the high-energy neutrons. At 30 cm behind the mockup on the reactor beam centerline, the 10-in. Bonner ball results indicate an attenuation of about 2.7×10^3. For the 5-in. Bonner ball, it is about the same, 2.5×10^3; for the Cd-covered detector it is a bit less, about 1.6×10^3; and for the bare detector it was approximately 2.3×10^2.

A detailed analysis of this experiment is reported by C. O. Slater in another report.[5]

REFERENCES

1. R. E. Maerker, L. R. Williams, F. R. Mynatt, and N. M. Greene, *Response Functions for Bonner Ball Neutron Detectors*, ORNL/TM-3451 (June 18, 1971).
2. C. E. Burgart and M. D. Emmett, *Monte Carlo Calculations of the Response Functions of Bonner Ball Neutron Detectors*, ORNL/TM-3739 (April 3, 1972).
3. B. W. Rust, D. T. Ingersoll, and W. R. Burrus, *A User's Manual for the FERDO and FERD Unfolding Codes*, ORNL/TM-8720 (September 1983).
4. J. O. Johnson and D. T. Ingersoll, *User's Guide for the Revised SPEC-4 Neutron Spectrum Unfolding Code*, ORNL/TM-7384 (August 1980).
5. C. O. Slater, *Analysis of Phase I of the HTGR Bottom Reflector and Core Support Block Neutron-Streaming Experiment*, ORNL/TM-9252 (1984).

APPENDIX A

EXPERIMENTAL PROGRAM PLAN FOR THE HTGR BOTTOM REFLECTOR AND SUPPORT BLOCK NEUTRON STREAMING EXPERIMENT

Phase I Measurements

I. Spectrum Modifier

A. Spectrum modifier (SM) only (5.08 cm carbon steel + 30.48 cm graphite).

1. NE-213 and hydrogen counter measurements on centerline as close as feasible to the spectrum modifier (with 15.4 cm Fe between detector and SM).
2. 3-, 6-, and 10-in. Bonner ball measurements on centerline at same location as spectrometers with and without 15.4 cm Fe following configuration.
3. Bare, Cd-covered, 5-, and 10-in. Bonner ball measurements:
   a. Horizontal traverses at 30 cm beyond configuration.
4. Bare, Cd-covered, and 5-in. Bonner ball horizontal traverses as close as feasible behind spectrum modifier.

AA. Spectrum modifier + 15 cm void + upper boron pin layer (770 boronated graphite (BG) + 738 graphite pins).

1. Bare, Cd-covered, and 5-in. Bonner ball traverses in horizontal plane as close as feasible behind spectrum modifier.

II. Reference Pattern of Boron Pins in Upper Shield Layer

A. Spectrum modifier + upper boron pin layer (770 BG + 738 graphite pins).

1. NE-213 and hydrogen counter measurements on centerline as close as feasible to the configuration (with 15.4 cm Fe between detector and configuration).
2. 3-, 6-, and 10-in. Bonner ball measurements on centerline at same location as spectrometers with and without 15.4 cm of Fe following configuration.
3. Bare, Cd-covered, 5-, and 10-in. Bonner ball measurements:
   a. Horizontal traverses at 30 cm beyond configuration.
   b. On centerline at 300 cm beyond configuration.
4. Bare and Cd-covered Bonner ball horizontal traverses as close as feasible to configuration.
5. 5-in. Bonner ball vertical traverse at 30 cm beyond the configuration.

AA. Spectrum modifier + upper boron pin layer (770 BG + 738 graphite pins) + boral shroud.

1. Bare and Cd-covered Bonner ball horizontal traverses as close as feasible behind the configuration.

AAA. Spectrum modifier + upper boron pin layer (770 BG + 738 graphite pins) + 15 cm void + reflector layer of graphite.

1. Bare and Cd-covered Bonner ball traverses in horizontal plane in 15 cm void as close as feasible to upper boron pin layer.

AAAA. Spectrum modifier + upper boron pin layer (770 BG + 738 graphite pins) + boral shroud + 15 cm void + reflector layer of graphite.

1. Bare and Cd-covered Bonner ball traverses in horizontal plane in 15 cm void as close as feasible behind upper boron pin layer.

B. Spectrum modifier + upper boron pin layer (770 BG + 738 graphite pins) + boral shroud + reflector layer.

1. Bare, Cd-covered, 5-, and 10-in. Bonner ball measurements:
   a. Horizontal traverses at 30 cm beyond configuration.
   b. On centerline at 300 cm beyond configuration.
2. Bare and Cd-covered Bonner ball horizontal traverses as close as feasible behind the configuration.

BB. Spectrum modifier + upper boron pin layer (770 BG + 738 graphite pins) + boral shroud + reflector layer + 15 cm void + layer C (crossover layer).

1. Bare and Cd-covered Bonner ball horizontal traverses in 15 cm void as close as feasible behind the reflector layer.

C. Spectrum modifier + upper boron pin layer (770 BG + 738 graphite pins) + boral shroud + reflector layer + crossover layer.

1. Bare, Cd-covered, 5-, and 10-in. Bonner ball measurements:
   a. Horizontal traverses at 30 cm beyond configuration.
   b. On centerline at 300 cm beyond configuration.
2. Bare and Cd-covered Bonner ball horizontal traverses as close as feasible behind the configuration.

CC. Spectrum modifier + upper boron pin layer shield (770 BG + 738 graphite pins) + boral shroud + reflector layer + crossover layer + 15 cm void + section D layer.

1. Bare and Cd-covered Bonner ball horizontal traverses in 15 cm void as close as feasible behind the crossover layer.

D. Spectrum modifier + upper boron pin layer (770 BG + 738 graphite pins) + boral shroud + reflector layer + crossover layer + section D layer.

1. Bare, Cd-covered, 5-, and 10-in. Bonner ball measurements:
   a. Horizontal traverses at 30 cm beyond configuration.
   b. On centerline at 300 cm beyond configuration.
2. Bare and Cd-covered Bonner ball axial traverses into one 19.18-cm-diameter coolant hole.
3. Bare and Cd-covered Bonner ball horizontal traverses as close as feasible behind the configuration.

III. Full Pattern of Boron Pins in Upper Shield Layer

A. Spectrum modifier + upper boron pin layer (1508 BG pins).

1. NE-213 and hydrogen counter measurements on centerline as close as feasible to the configuration (with 15.4 cm Fe between detector and configuration).
2. 3-, 6-, and 10-in. Bonner ball measurements on centerline at same location as spectrometer with and without 15.4 cm Fe following configuration.

3. Bare, Cd-covered, 5-, and 10-in. Bonner ball measurements:
    a. Horizontal traverses at 30 cm beyond configuration.
    b. On centerline at 300 cm beyond configuration.
4. Bare and Cd-covered Bonner ball horizontal traverses as close as feasible to configuration.
5. 5-in. Bonner ball vertical traverses at 30 cm beyond the configuration.

AA. Spectrum modifier + upper boron pin layer (1508 BG pins) + boral shroud.

1. Bare and Cd-covered Bonner ball horizontal traverses as close as feasible behind configuration.

AAA. Spectrum modifier + upper boron pin layer (1508 BG pins) + 15 cm void + reflector layer of graphite.

1. Bare and Cd-covered Bonner ball horizontal traverses in 15 cm void as close as feasible to upper boron pin layer.

AAAA. Spectrum modifier + upper boron pin layer (1508 BG pins) + boral shroud + 15 cm void + reflector layer of graphite.

1. Bare and Cd-covered Bonner ball horizontal traverses in 15 cm void as close as feasible behind upper boron pin layer.

B. Spectrum modifier + upper boron pin layer (1508 BG pins) + boral shroud + reflector layer.

1. Bare, Cd-covered, 5-, and 10-in. Bonner ball measurements:
    a. Horizontal traverses at 30 cm beyond configuration.
    b. On centerline at 300 cm beyond configuration.
2. Bare and Cd-covered Bonner ball horizontal traverses as close as feasible behind the configuration.

BB. Spectrum modifier + upper boron pin layer (1508 BG pins) + boral shroud + reflector layer + 15 cm void + layer C (crossover layer).

1. Bare and Cd-covered Bonner ball horizontal traverses in 15 cm void as close as feasible behind the reflector layer.

C. Spectrum modifier + upper boron pin layer (1508 BG pins) + boral shroud + reflector layer + crossover layer.

1. Bare, Cd-covered, 5-, and 10-in. Bonner ball measurements:
    a. Horizontal traverses at 30 cm beyond configuration.
    b. Centerline at 300 cm beyond configuration.
2. Bare and Cd-covered Bonner ball horizontal traverses as close as feasible behind the configuration.

CC. Spectrum modifier + upper boron pin layer (1508 BG pins) + boral shroud + reflector layer + crossover layer + 15 cm void + section D layer.

1. Bare and Cd-covered Bonner ball horizontal traverses in 15 cm void as close as feasible behind the crossover layer.

D. Spectrum modifier + upper boron pin layer (1508 BG pins) + boral shroud + reflector layer + crossover layer + section D layer.

1. Bare, Cd-covered, 5-, and 10-in. Bonner ball measurements:
   a. Horizontal traverses at 30 cm beyond configuration.
   b. On centerline at 300 cm beyond configuration.
2. Bare and Cd-covered Bonner ball axial traverses into one of the 19.18 cm diameter holes.
3. Bare and Cd-covered Bonner ball horizontal traverses as close as feasible behind the configuration.

APPENDIX B. TABLES OF DATA

LIST OF TABLES

Table 1. Analysis of iron slab used in spectrum modifier[a]

Element	wt %
Fe	98.4
C	0.25
Cr	0.15
Cu	0.03
Mn	1.0
Mo	0.02
Ni	0.05
Si	0.25

[a] $\rho = 7.86$ g/cc.

Table 2. Analysis of impurities in graphite pieces[a] (Pieces were 10.16 cm on a side by 121.9 cm long.)

Element	ppm	Element	ppm	Element	ppm
Ag	< 0.5	Ge	< 5	Sb	< 10
Al	12.5	Hg	< 10	Si	100
B	1.5	In	< 10	Sn	< 10
Ba	< 5	K	< 100	Sr	< 10
Be	< 0.5	Li	< 2	Ta	< 10
Bi	< 10	Mg	7.5	Te	< 25
Ca	150	Mn	< 1	Ti	30
Cd	< 25	Mo	< 5	V	100
Co	< 10	Na	< 5	W	< 5
Cr	< 10	Nb	< 5	Zn	10
Cu	7.5	Ni	< 10	Zr	< 5
Fe	50	Pb	< 5		
Ga	< 10	Rb	< 5		

[a] $\rho = 1.62$ g/cc.

Table 3. Composition of small concrete pieces[a] (Blocks were 15.2 cm on a side by 30.5 cm long.)

Element	Number density
Na	2.73 E-5[b]
O	4.202 E-2
Si	3.84 E-3
Mg	1.44 E-3
Fe	2.64 E-4
H	8.88 E-3
Al	4.14 E-4
Ca	1.00 E-2
K	2.34 E-3
C	7.97 E-3
S	1.015 E-4

[a] ρ = 2.39 g/cc.
[b] Read as 2.73×10^{-5}.

Table 4. Composition of large concrete blocks[a] (Blocks were 61 cm on a side and 30.5 cm thick.)

Element	wt %	Element	wt %
CO_3	41.9	Al_2O_3	2.2
Ca	27.4	Fe_2O_3	0.60
SiO_2	18.1	SO_3	0.32
H_2O	4.0	P_2O_5	0.035
Mg	3.66	K	0.30
O_2	1.4		

[a] ρ = 2.40 g/cc.

Table 5. ORNL analyses of boronated graphite pins and vendor's list of properties[a]

Element	Sample 1	Sample 2
	wt %	
B	22.57	27.42
C	77.62	73.26
	ppm	
Ag	< 9	< 8.6
Al	19000	16000
Ba	35	30
Be	< 0.65	< 0.62
Ca	1100	820
Cd	15	12
Co	< 6.5	< 6.2
Cr	36	39
Cu	280	23
Fe	3100	1800
Ga	< 35	< 33
K	2000	< 1900
Mg	240	220
Mn	31	19
Mo	43	93
Na	1300	1100
Ni	61	< 53
Pb	< 130	< 120
Sb	< 70	78
Se	420	380
Si	9500	8400
Sr	15	13
Ti	350	430
V	27	29
Zn	180	13
Zr	56	62
P	520	470

[a]Properties:
Diameter, 1.237 cm (0.487 in.).
Density, 1.54 g/cc.
Boron content, 24.3 w/o.
Trace impurities (mostly Fe, Si, Ca, Al), 0.45%.
% Boron in oxide, from 0.11 w/o.
Boron density, 0.375 g B/cc.

Table 6. Analyses of graphite segments and graphite[a] pins used in mockup (Segments were 55.88 cm square.)

Element	Sample 1	Sample 2	Sample 3
		wt %	
C	99.85	99.92	99.85
		ppm	
Ag	< 0.22	< 0.22	< 0.17
Al	27	< 0.69	1.8
Be	< 0.016	< 0.016	0.012
Ca	160	24	44
Cd	0.45	0.32	0.27
Co	< 0.16	< 0.16	< 0.12
Cr	< 0.28	< 0.28	0.21
Cu	0.4	< 0.38	0.72
Fe	170	8.7	77
K	< 49	< 48	< 37
Mg	1.2	< 0.19	< 0.15
Mn	0.46	0.091	0.64
Ni	< 1.4	< 1.3	1.3
Pb	< 3.2	< 3.1	< 2.4
Si	11	< 1.4	29
Ti	15	4.2	9.9
V	11	0.57	4.3
Zn	8.9	1.6	1.6
Zr	1	1.1	0.87
P	< 4.1	< 3.9	< 3

[a] ρ = 1.75 g/cc.

Table 7. Properties of boral in shroud

Percent boron carbide in core	35 w/o (min)
Core density	2.64 g/cc
Core minimum thickness	4.32 mm
Outer aluminum sheet thickness	1.04 mm
Total thickness plus tolerance	6.7 ± 0.4 mm
Average wt/unit area of plate	17.82 kg/m^2

Analysis of core

Element	wt %
B (natural)	25.2
C	8.6
Al	65.0
Fe and other	1.2

Table 8. Distances from the backs of the configurations to the center of the reactor

Configuration	Distance (cm)
Item I A, spectrum modifier	127.7
Configuration with reference pattern BP layer	
Item II A, BP layer	148.1
Item II B, reflector layer	171.8
Item II C, crossover layer	212.4
Item II D, follow-on layer	248.3
Configuration with full pattern BP layer	
Item III A, BP layer	148.2
Item III B, reflector layer	172.0
Item III C, crossover layer	213.0
Item III D, follow-on layer	248.8

Table 9. Fast-neutron fluxes (>0.8 MeV) on centerline 125.4 cm beyond spectrum modifier (Item I A): Run 7831A

Neutron energy (MeV)	Flux (neutrons cm^{-2} MeV^{-1} kW^{-1} s^{-1}) Lower limit	Upper limit	Neutron energy (MeV)	Flux (neutrons cm^{-2} MeV^{-1} kW^{-1} s^{-1}) Lower limit	Upper limit
8.1135E−01[a]	3.7495E+04	3.7973E+04	5.9380E+00	6.6195E+02	6.9231E+02
9.0694E−01	4.1739E+04	4.1987E+04	6.2542E+00	6.0872E+02	6.4817E+02
1.0066E+00	3.7450E+04	3.7644E+04	6.5557E+00	5.5095E+02	5.8396E+02
1.1069E+00	3.1924E+04	3.2110E+04	6.8390E+00	4.7485E+02	4.9739E+02
1.2047E+00	2.6733E+04	2.6895E+04	7.2352E+00	3.5051E+02	3.6947E+02
1.3096E+00	2.1825E+04	2.1973E+04	7.7365E+00	2.2649E+02	2.4707E+02
1.4121E+00	1.8351E+04	1.8496E+04	8.2364E+00	1.6929E+02	1.8724E+02
1.5107E+00	1.6002E+04	1.6134E+04	8.7578E+00	1.4252E+02	1.5551E+02
1.6100E+00	1.4089E+04	1.4205E+04	9.2613E+00	1.1357E+02	1.2484E+02
1.7095E+00	1.2312E+04	1.2421E+04	9.7411E+00	8.3102E+01	9.4006E+01
1.8125E+00	1.0627E+04	1.0731E+04	1.0259E+01	6.2057E+01	7.1661E+01
1.9323E+00	8.9702E+03	9.0683E+03	1.0777E+01	5.2341E+01	6.0885E+01
2.1000E+00	7.0510E+03	7.1411E+03	1.1247E+01	4.4542E+01	5.2472E+01
2.2961E+00	5.2108E+03	5.2959E+03	1.1751E+01	3.7257E+01	4.4359E+01
2.4988E+00	3.8351E+03	3.9025E+03	1.2393E+01	3.2426E+01	3.8723E+01
2.7026E+00	2.8713E+03	2.9427E+03	1.3201E+01	2.6569E+01	3.1464E+01
2.8984E+00	2.2706E+03	2.3400E+03	1.4021E+01	1.6372E+01	1.9953E+01
3.0975E+00	1.7880E+03	1.8629E+03	1.4792E+01	7.6443E+00	1.0573E+01
3.2965E+00	1.3890E+03	1.4474E+03	1.5629E+01	1.8243E+00	4.4275E+00
3.5009E+00	1.1378E+03	1.2083E+03	1.6539E+01	−4.1978E−01	1.7074E+00
3.7074E+00	1.0651E+03	1.1216E+03	1.7533E+01	−1.1442E+00	9.0104E−01
3.9061E+00	1.0756E+03	1.1241E+03	1.8521E+01	−1.4079E+00	9.5142E−01
4.1528E+00	1.0820E+03	1.1305E+03	1.9498E+01	−1.2028E+00	1.0835E+00
4.4540E+00	1.0612E+03	1.1026E+03	2.0556E+01	−1.1880E+00	1.1048E+00
4.7521E+00	1.0533E+03	1.0927E+03	2.1580E+01	−9.0292E−01	1.2922E+00
5.0422E+00	9.8568E+02	1.0200E+03	2.2560E+01	−1.0615E+00	1.1957E+00
5.3459E+00	8.5345E+02	8.8624E+02	2.3471E+01	−1.1306E+00	1.3088E+00
5.6453E+00	7.3371E+02	7.6879E+02			

E1 (MeV)	E2 (MeV)	Integral (neutrons cm^{-2} kW^{-1} s^{-1})	Error (neutrons cm^{-2} kW^{-1} s^{-1})
0.811	1.000	7.6492E+03	2.6243E+01
1.000	1.200	6.4862E+03	1.8363E+01
1.200	1.600	7.7726E+03	2.8425E+01
1.600	2.000	4.4040E+03	2.0970E+01
2.000	3.000	4.2930E+03	3.8495E+01
3.000	4.000	1.3225E+03	3.0703E+01
4.000	6.000	1.8991E+03	3.7771E+01
6.000	8.000	8.6784E+02	2.5634E+01
8.000	10.000	2.6904E+02	1.3200E+01
10.000	12.000	1.0734E+02	8.3186E+00
12.000	16.000	7.6491E+01	8.1232E+00
16.000	20.000	4.7107E−01	4.4328E+00
1.500	15.000	1.4767E+04	1.8825E+02
3.000	12.000	4.4649E+03	1.1565E+02

[a]Read: 8.1135 × 10^{-1}.

Table 10. Neutron fluxes (50 keV to 1.4 MeV) on centerline 125.4 cm beyond spectrum modifier (Item I A): Runs 1503A, 1502A, 1501B

N	Energy boundary (MeV)		Flux (neutrons cm^{-2} MeV^{-1} kW^{-1} s^{-1})	Error (%)
1	0.0449	0.0524	3.92E 05[a]	4.91
2	0.0524	0.0637	3.23E 05	4.48
3	0.0637	0.0730	4.12E 05	4.94
4	0.0730	0.0861	4.24E 05	3.69
5	0.0861	0.1030	2.66E 05	5.02
6	0.1030	0.1198	2.63E 05	5.92
7	0.1198	0.1423	3.63E 05	3.43
8	0.1423	0.1666	2.80E 05	4.56
9	0.1666	0.1966	2.38E 05	4.65
10	0.1966	0.2303	1.76E 05	6.13
1	0.1690	0.1957	2.29E 05	1.96
2	0.1957	0.2312	1.77E 05	2.07
3	0.2312	0.2713	1.62E 05	2.25
4	0.2713	0.3202	1.99E 05	1.63
5	0.3202	0.3780	1.73E 05	1.68
6	0.3780	0.4447	1.07E 05	2.52
1	0.3192	0.3831	1.64E 05	0.66
2	0.3831	0.4469	1.07E 05	1.12
3	0.4469	0.5290	8.96E 04	1.11
4	0.5290	0.6202	1.02E 05	0.96
5	0.6202	0.7296	9.46E 04	0.87
6	0.7296	0.8573	5.68E 04	1.27
7	0.8573	1.0124	4.57E 04	1.31
8	1.0124	1.1857	3.48E 04	1.57
9	1.1857	1.3954	2.50E 04	1.74

[a]Read: 3.92×10^5.

Table 11. Bonner ball measurements at same locations as spectral measurements (Items I A, II A, III A)

Item	Shield Configuration	Distance on Centerline	Bonner ball count rate ($s^{-1}W^{-1}$)					
			3-in.-diam ball		6-in.-diam ball		10-in.-diam ball	
			Foreground[a]	Background[b]	Foreground	Background	Foreground	Background
I-A-2	Spectrum modifier (SM)	125.4 cm behind SM	6.52 (2)[c]	4.62 (1)	1.22 (3)	7.31 (1)	4.39 (2)	2.01 (1)
I-A-2	SM + 35 cm void + 15.4 cm Fe	125.4 cm behind SM	1.14 (2)	2.07 (1)	3.56 (2) 3.65 (2)	3.44 (1)	1.40 (2)	9.31 (0)
II-A-2	SM + upper pin layer (770 boronated + 738 graphite pins)	134.5 cm behind upper pin layer	7.57 (1)	6.41 (0)	1.67 (2)	9.53 (0)	6.77 (1)	3.28 (0)
II-A-2	SM + upper pin layer (770 boronated + 738 graphite pins) + 35 cm void + 15.4 cm Fe	134.5 cm behind upper pin layer	1.26 (1)	2.31 (0)	4.88 (1)	4.11 (0)	2.00 (1)	1.21 (0)
III-A-2	SM + upper pin layer (1508 boronated pins)	125.5 cm behind upper pin layer	6.06 (1)	4.36 (0)	1.47 (2)	7.20 (0)	6.63 (1)	1.99 (0)
III-A-2	SM + upper pin layer (1508 boronated pins) + 35 cm void + 15.4 cm Fe	125.5 cm behind upper pin layer	1.08 (1)	1.64 (0)	4.72 (1)	3.01 (0)	2.18 (1)	9.08 (-1)

[a]Neutron flux without shadow shield between detector and configuration.

[b]Neutron flux with shadow shield between detector and configuration.

[c]Read: 6.52×10^2.

Table 12. Bonner ball horizontal traverses close behind spectrum modifier[a] (Item I A)

Distance from Centerline (cm)	Bonner ball count rates ($s^{-1}W^{-1}$)		
	Bare counter[b]	Cd-covered counter[c]	5-in.-diam ball[d]
74.2 S	1.93 (3)[e]		
73.7		8.32 (1)	
73.5			1.77 (3)
64.2	3.02 (3)		
63.7		1.42 (2)	
63.5			2.98 (3)
54.2	4.42 (3,		
53.7		2.19 (2)	
53.5			4.58 (3)
44.2	5.65 (3)		
43.7		2.98 (2)	
43.5			6.50 (3)
34.2	6.78 (3)		
33.7		3.87 (2)	
33.5			8.04 (3)
24.2	7.98 (3)		
23.7		4.51 (2)	
23.5			9.48 (3)
14.2	8.58 (3)		
	7.78 (3)		
13.7		4.94 (2)	
13.5			1.07 (4)
4 2	8.94 (3)		
	8.66 (3)		
3.7		5.19 (2)	
3.5			1.03 (4)
5.8	9.14 (3)		
	9.25 (3)		
6.3		5.7 (2)	
6.5			1.11 (4)
15.8	8.98 (3)		
16.3		4.78 (2)	
16.5			9.91 (3)
25.8	8.06 (3)		
26.3		4.32 (2)	
26.5			9.47 (3)
35.8	6.83 (3)		
36.3		3.63 (2)	
36.5			7.67 (3)
45.8	5.59 (3)		
46.3		2.76 (2)	
46.5			5.65 (3)
55.8	4.09 (3)		
56.3		1.96 (2)	
56.5			3.89 (3)
65.8	2.81 (3)		
66.3		1.22 (2)	
66.5			2.46 (3)
71.8	2.32 (3)		
73.8		8.43 (1)	
74.0 N			1.66 (3)

[a] Traverses within horizontal midplane of configuration.
[b] 4.3 cm behind configuration.
[c] 4 cm behind configuration.
[d] 7.62 cm behind configuration.
[e] Read: 1.93×10^3.

Table 13. Bonner ball horizontal traverses 30 cm beyond spectrum modifier[a] (Item I A)

Distance from Centerline (cm)	Bonner ball count rates ($s^{-1}W^{-1}$)			
	Bare counter	Cd-covered counter	5-in.-diam ball	10-in.-diam ball
73.7 S			1.91 (3)[b]	
73.4				5.92 (2)
73.2	1.99 (3)	8.84 (1)		
63.7			2.60	
63.4				8.03 (2)
63.2	2.56 (3)	1.26 (2)		
53.7			3.38 (3)	
53.4				1.06 (3)
53.2	3.21 (3)	1.60 (2)		
43.7			4.04 (3)	
43.4				1.35 (3)
43.2	3.69 (3)	1.96 (2)		
33.7			5.03 (3)	
33.4				1.54 (3)
33.2	4.42 (3)	2.31 (2)		
	4.28 (3)			
23.7			5.68 (3)	
23.4				1.78 (3)
23.2	4.77 (3)	2.59 (2)		
13.7			6.15 (3)	
13.4				1.93 (3)
13.2	5.12 (3)	2.84 (2)		
3.7			6.37 (3)	
3.4				2.01 (3)
3.2	5.26 (3)	2.90 (2)		
	5.41 (3)			
6.3			6.46 (3)	
6.6				2.00 (3)
6.8	5.21 (3)	2.84 (2)		
	5.40 (3)			
16.3			6.03 (3)	
16.6				1.84 (3)
16.8	5.07 (3)	2.71 (2)		
	5.19 (3)			
26.3			5.70 (3)	
26.6				1.72 (3)
26.8	4.60 (3)	2.51 (2)		
36.3			5.14 (3)	
36.6				1.49 (3)
36.8	4.18 (3)	2.16 (2)		
46.3			3.90 (3)	
46.6				1.23 (3)
46.8	3.50 (3)	1.82 (2)		
56.3			3.14 (3)	
56.6				9.98 (2)
56.8	2.94 (3)	1.49 (2)		
66.3			2.38 (3)	
66.6				7.53 (2)
66.8	2.34 (3)	1.15 (2)		
71.6				6.28 (2)
73.8 N	1.90 (3)	9.19 (1)	2.08 (3)	

[a]Traverses within horizontal midplane of configuration.
[b]Read: 1.91×10^{3}.

Table 14. Bonner ball horizontal traverses within 15-cm-thick void between spectrum modifier and boron pin layer[a] (Item I AA, reference pin pattern)

Distance from Centerline (cm)	Bonner ball count rates ($s^{-1}W^{-1}$)		
	Bare counter[b]	Cd-covered counter[c]	5-in.-diam ball[d]
73.2 S		2.61 (2)[e]	
72.7	6.76 (3)		
70			6.02 (3)
63.2		3.86 (2)	
62.7	9.16 (3)		
60			8.46 (3)
53.2		5.09 (2)	
52.7	1.11 (4)		
50			1.19 (4)
43.2		6.12 (2)	
42.7	1.22 (4)		
40			1.43 (4)
33.2		7.25 (2)	
32.7	1.34 (4)		
30			1.70 (4)
23.2		7.98 (2)	
22.7	1.46 (4)		
20			2.01 (4)
13.2		8.62 (2)	
12.7	1.58 (4)		
10			2.01 (4)
3.2		9.01 (2)	
2.7	1.64 (4)		
0			2.09 (4)
6.8		8.96 (2)	
7.3	1.65 (4)		
10			1.98 (4)
16.8		8.46 (2)	
17.3	1.50 (4)		
20			2.07 (4)
26.8		7.81 (2)	
27.3	1.45 (4)		
30			1.68 (4)
36.8		6.88 (2)	
37.3	1.25 (4)		
40			1.41 (4)
46.8		5.84 (2)	
47.3	1.10 (4)		
50			1.17 (4)
56.8		4.54 (2)	
57.3	1.03 (4)		
60			8.63 (3)
66.8		3.27 (2)	
67.3	8.02 (3)		
70			5.76 (3)
73.8		2.43 (2)	
74.3 N	5.85 (3)		

[a] Traverses within horizontal midplane of configuration.
[b] 4 cm behind configuration.
[c] 4.3 cm behind configuration.
[d] 7.3 cm behind configuration.
[e] Read: 2.61×10^2.

Table 15. Fast-neutron fluxes (>0.8 MeV) on centerline 134.5 cm beyond boron pin layer (Item II A, reference pin pattern): Run 7833B

Neutron energy (MeV)	Flux (neutrons cm^{-2} MeV^{-1} kW^{-1} s^{-1})		Neutron energy (MeV)	Flux (neutrons cm^{-2} MeV^{-1} kW^{-1} s^{-1})	
	Lower limit	Upper limit		Lower limit	Upper limit
8.1135E−01[a]	5.8282E+03	5.9119E+03	5.9380E+00	1.6376E+02	1.7044E+02
9.0694E−01	6.3615E+03	6.4054E+03	6.2542E+00	1.5414E+02	1.6290E+02
1.0066E+00	5.7057E+03	5.7399E+03	6.5557E+00	1.4446E+02	1.5170E+02
1.1069E+00	4.8664E+03	4.8996E+03	6.8390E+00	1.2491E+02	1.2989E+02
1.2047E+00	4.0846E+03	4.1135E+03	7.2352E+00	9.0973E+01	9.5003E+01
1.3096E+00	3.3548E+03	3.3815E+03	7.7365E+00	6.0512E+01	6.5012E+01
1.4121E+00	2.8208E+03	2.8474E+03	8.2364E+00	4.4904E+01	4.8746E+01
1.5107E+00	2.4609E+03	2.4852E+03	8.7578E+00	3.5200E+01	3.7933E+01
1.6100E+00	2.1893E+03	2.2106E+03	9.2613E+00	2.5452E+01	2.7779E+01
1.7095E+00	1.9487E+03	1.9688E+03	9.7411E+00	1.9708E+01	2.1980E+01
1.8125E+00	1.7092E+03	1.7284E+03	1.0259E+01	1.6545E+01	1.8542E+01
1.9323E+00	1.4500E+03	1.4683E+03	1.0777E+01	1.3842E+01	1.5572E+01
2.1000E+00	1.1439E+03	1.1609E+03	1.1247E+01	1.1394E+01	1.2990E+01
2.2961E+00	8.4765E+02	8.6404E+02	1.1751E+01	8.7107E+00	1.0053E+01
2.4988E+00	6.2550E+02	6.3845E+02	1.2393E+01	6.0293E+00	7.1902E+00
2.7026E+00	4.8309E+02	4.9740E+02	1.3201E+01	4.9430E+00	5.7489E+00
2.8984E+00	3.8686E+02	4.0081E+02	1.4021E+01	3.6981E+00	4.2717E+00
3.0975E+00	3.1028E+02	3.2540E+02	1.4792E+01	1.9462E+00	2.3797E+00
3.2965E+00	2.5308E+02	2.6492E+02	1.5629E+01	5.2597E−01	9.0204E−01
3.5009E+00	2.1120E+02	2.2562E+02	1.6539E+01	−6.4077E−02	2.4291E−01
3.7074E+00	1.9569E+02	2.0742E+02	1.7533E+01	−2.1260E−01	8.1868E−02
3.9061E+00	2.0034E+02	2.1041E+02	1.8521E+01	−2.3309E−01	1.0636E−01
4.1528E+00	2.1291E+02	2.2306E+02	1.9498E+01	−1.8660E−01	1.4226E−01
4.4540E+00	2.2563E+02	2.3439E+02	2.0556E+01	−1.7693E−01	1.5274E−01
4.7521E+00	2.2933E+02	2.3777E+02	2.1580E+01	−1.3640E−01	1.7906E−01
5.0422E+00	2.1446E+02	2.2194E+02	2.2560E+01	−1.5920E−01	1.6485E−01
5.3459E+00	1.9304E+02	2.0021E+02	2.3471E+01	−1.6616E−01	1.8424E−01
5.6453E+00	1.7680E+02	1.8458E+02			

E1 (MeV)	E2 (MeV)	Integral (neutrons cm^{-2} kW^{-1} s^{-1})	Error (neutrons cm^{-2} kW^{-1} s^{-1})
0.811	1.000	1.1700E+03	4.6292E+00
1.000	1.200	9.8940E+02	3.2670E+00
1.200	1.600	1.1953E+03	5.1745E+00
1.600	2.000	7.0265E+02	3.8795E+00
2.000	3.000	7.0601E+02	7.4934E+00
3.000	4.000	2.4069E+02	6.2830E+00
4.000	6.000	4.1621E+02	8.1394E+00
6.000	8.000	2.2407E+02	5.6059E+00
8.000	10.000	6.5770E+01	2.7773E+00
10.000	12.000	2.7047E+01	1.6721E+00
12.000	16.000	1.5287E+01	1.3376E+00
16.000	20.000	−5.2826E−04	6.3833E−01
1.500	15.000	2.6327E+03	3.8169E+01
3.000	12.000	9.7344E+02	2.4485E+01

[a]Read: 8.1135×10^{-1}.

Table 16. Neutron fluxes (50 keV to 1.4 MeV) on centerline 134.5 cm beyond boron pin layer (Item II A, reference pin pattern): Runs 1506A, 1508C, and 1505A

N	Energy boundary (MeV)		Flux (neutrons cm^{-2} MeV^{-1} kW^{-1} s^{-1})	Error (%)
1	0.0449	0.0524	6.49E 04[a]	4.47
2	0.0524	0.0636	4.54E 04	4.80
3	0.0636	0.0729	6.03E 04	5.09
4	0.0729	0.0860	6.00E 04	3.95
5	0.0860	0.1028	3.66E 04	5.54
6	0.1028	0.1197	4.01E 04	5.92
7	0.1197	0.1421	5.42E 04	3.50
8	0.1421	0.1664	3.98E 04	4.91
9	0.1664	0.1963	3.78E 04	4.51
10	0.1963	0.2300	2.70E 04	6.16
1	0.1668	0.1967	3.77E 04	1.86
2	0.1967	0.2309	2.18E 04	3.15
3	0.2309	0.2737	2.41E 04	2.52
4	0.2737	0.3207	3.02E 04	2.04
5	0.3207	0.3763	2.61E 04	2.12
6	0.3763	0.4448	1.64E 04	2.89
1	0.3192	0.3831	2.38E 04	0.82
2	0.3831	0.4469	1.63E 04	1.35
3	0.4469	0.5290	1.42E 04	1.30
4	0.5290	0.6202	1.63E 04	1.11
5	0.6202	0.7296	1.54E 04	1.00
6	0.7296	0.8573	9.30E 03	1.44
7	0.8573	1.0124	7.48E 03	1.50
8	1.0124	1.1857	5.79E 03	1.77
9	1.1857	1.3954	4.13E 03	1.99

[a]Read: 6.49×10^4.

Table 17. 5-in.-diameter Bonner ball vertical traverses 30 cm beyond boron pin layers[a] (Item II A, reference pin pattern; and Item III A, full pin pattern)

Distance from Centerline (cm)	Bonner ball count rates (s^{-1} W^{-1})	
	Reference pin pattern, Item II A[b]	Full pin pattern, Item III A[c]
76.2 Above	2.32 (2)[d]	
71.2	2.68 (2)	
70		2.36 (2)
66.2	3.10 (2)	
61.2	3.49 (2)	
60		3.01 (2)
56.2	3.90 (2)	
51.2	4.44 (2)	
50		3.55 (2)
46.2	4.78 (2)	
41.2	5.32 (2)	
40		4.23 (2)
36.2	5.61 (2)	
31.2	6.07 (2)	
30		4.54 (2)
26.2	6.27 (2)	
21.2	6.61 (2)	
20		5.03 (2)
16.2	6.86 (2)	
11.2	7.00 (2)	
10		5.27 (2)
6.2	7.15 (2)	
1.2	7.19 (2)	
0	7.09 (2)	5.41 (2)
3.8	7.31 (2)	
8.8	7.33 (2)	
10		5.53 (2)
13.8	7.15 (2)	
18.8	7.18 (2)	
20		5.48 (2)
28.8	6.74 (2)	
30		5.31 (2)
38.8	6.27 (2)	
40		4.92 (2)
47.5		4.56 (2)
48.8	5.35 (2)	
58.8	4.48 (2)	
68.8	3.60 (2)	
72.8 Below	3.24 (2)	

[a]Traverses within vertical midplane of configuration.
[b]SM + upper boron pin layer (770 BG + 738 graphite pins).
[c]SM + upper boron pin layer (1508 BG pins).
[d]Read: 2.32×10^2.

Table 18. Bonner ball horizontal traverses close behind boron pin layer with and without boral shroud[a] (Item II A, AA; reference pin pattern)

Distance from Centerline (cm)	Bonner ball count rates ($s^{-1}W^{-1}$)			
	Without boral shroud		With boral shroud	
	Bare counter[b]	Cd-covered counter[c]	Bare counter[b]	Cd-covered counter[d]
73.2 S	7.99 (2)[e]	1.78 (1)		
71.2			4.87 (1)	
70				4.72 (0)
68.2	9.38 (2)			
66.2			3.35 (1)	
63.2	9.28 (2)	2.51 (1)		
61.2			3.82 (1)	
60				6.77 (0)
58.2	7.98 (2)	2.47 (1)		
56.2			5.23 (1)	
53.2	5.57 (2)	2.12 (1)		
52.2	5.09 (2)			
51.2			1.43 (2)	
46.2			1.29 (2)	
45				1.21 (1)
43.2	2.40 (2)	1.54 (1)		
36.2			8.13 (1)	
33.2	1.73 (2)	1.58 (1)		
30				1.38 (1)
26.2			7.10 (1)	
23.2	1.47 (2)	1.67 (1)		
16.2			6.94 (1)	
15.0				1.55 (1)
13.2	1.40 (2)	1.73 (1)		
3.2	1.35 (2)	1.70 (1)		
0			5.91 (1)	1.46 (1)
6.8	1.39 (2)	1.76 (1)		
16.8	1.48 (2)	1.72 (1)		
26.8	1.56 (2)	1.61 (1)		
36.8	1.93 (2)	1.54 (1)		
46.8	3.27 (2)	1.62 (1)		
51.8		1.95 (1)		
56.8	7.57 (2)	2.27 (1)		
61.8	9.49 (2)	2.45 (1)		
66.8	1.01 (3)	2.28 (1)		
73.8 N	8.38 (2)	1.72 (1)		

[a]Traverses within horizontal midplane of configuration.
[b]Detector at 4 cm behind mockup.
[c]Detector at 3.8 cm behind mockup.
[d]Detector at 4.8 cm behind mockup.
[e]Read: 7.99×10^2.

Table 19. Bonner ball horizontal traverses 30 cm beyond boron pin layer[a] (Item II A, reference pin pattern)

Distance from Centerline (cm)	Bonner ball count rates ($s^{-1}W^{-1}$)			
	Bare counter	Cd-covered counter	5-in.-diam ball	10-in.-diam ball
73.2 S	4.56 (2)[b]	1.19 (1)	2.98 (2)	1.00 (2)
63.2	4.96 (2)	1.39 (1)	3.78 (2)	1.37 (2)
53.2	4.86 (2)	1.55 (1)	4.69 (2)	1.73 (2)
43.2	4.44 (2)	1.61 (1)	5.67 (2)	2.13 (2)
33.2	4.00 (2)	1.61 (1)	6.41 (2)	2.47 (2)
23.2	3.52 (2)	1.59 (1)	7.19 (2)	2.71 (2)
13.2	3.21 (2)	1.57 (1)	7.50 (2)	2.91 (2)
3.2	3.08 (2)	1.52 (1)	7.56 (2)	2.95 (2)
6.8	3.14 (2)	1.56 (1)	7.52 (2)	2.95 (2)
16.8	3.33 (2)	1.57 (1)	7.30 (2)	2.85 (2)
26.8	3.72 (2)	1.60 (1)	6.98 (2)	2.67 (2)
36.8	4.28 (2)	1.59 (1)	6.18 (2)	2.37 (2)
46.8	4.83 (2)	1.60 (1)	5.35 (2)	2.00 (2)
56.8	5.16 (2)	1.46 (1)	4.36 (2)	1.60 (2)
66.8	5.11 (2)	1.30 (1)	3.42 (2)	1.23 (2)
73.8 N	4.71 (2)	1.16 (1)	2.88 (2)	9.94 (1)

[a]Traverses within horizontal midplane of configuration.
[b]Read: 4.56×10^2.

Table 20. Bonner ball measurements on beam centerline 300 cm beyond various configurations (Items II A-D, III A-d)

Configuration[a]	Bare counter		Cd-covered counter		5-in.-diam ball		10-in.-diam ball	
	Foreground[b]	Background[c]	Foreground	Background	Foreground	Background	Foreground	Background
			Boronated and graphite pins in upper pin layer (reference pin pattern)					
Item II A	5.78 (1)[d]	1.24 (1)	1.81 (0)	3.10 (-1)	4.92 (1)	6.20 (0)	1.91 (1)	1.66 (0)
Item II B	4.78 (0)	1.28 (0)	4.09 (-1)	6.73 (-2)	9.03 (0)	1.04 (0)	3.55 (0)	2.80 (-1)
Item II C	3.97 (0)	7.59 (-1)	9.78 (-2)	1.00 (-2)	1.75 (0)	1.39 (-1)	6.45 (-1)	3.44 (-2)
Item II D	2.30 (0)	3.65 (-1)	4.64 (-2)	3.83 (-3)	8.26 (-1)	4.89 (-2)	2.99 (-1)	1.12 (-2)
			Boronated pins only in upper pin layer (full pin pattern)					
Item III A	4.86 (1)	9.25 (0)	1.39 (0)	2.20 (-1)	3.89 (1)	4.39 (0)	1.71 (1)	1.29 (0)
Item III B	3.37 (0)	1.19 (0)	3.17 (-1)	5.60 (-2)	7.61 (0)	9.66 (-1)	3.27 (0)	2.79 (-1)
Item III C	2.81 (0)	6.43 (-1)	7.77 (-2)	1.08 (-2)	1.53 (0)	1.56 (-1)	5.94 (-1)	3.80 (-2)
Item III D	1.75 (0)	2.98 (-1)	3.54 (-2)	4.20 (-3)	7.45 (-1)	6.47 (-2)	2.90 (-1)	1.42 (-2)
Item III D			3.82 (-2)	4.55 (-3)				

[a] See experimental program plan in Appendix A for description of configurations.
[b] Neutron flux without shadow shield between detector and configuration.
[c] Neutron flux with shadow shield between detector and configuration.
[d] Read: 5.78×10^{1}.

Table 21. Bonner ball horizontal traverses within 15-cm-thick void between boron pin layer and reflector layer with and without boral shroud[a] (Items II AAA, AAAA; reference pin pattern)

Distance from Centerline (cm)	Bonner ball count rate ($s^{-1}W^{-1}$)			
	Without boral shroud		With boral shroud	
	Bare counter[b]	Cd-covered counter[c]	Bare counter[d]	Cd-covered counter
72.2 S			1.35 (2)[e]	
70.2				1.58 (1)
67.2			1.09 (2)	
65.2		5.75 (1)		1.92 (1)
64.2	2.05 (3)			
62.2			1.22 (2)	
60.2				2.29 (1)
59.2	1.97 (3)			
57.2			1.45 (2)	
55.2		6.10 (1)		2.83 (1)
54.2	1.76 (3)			
52.2			2.48 (2)	
50.2				3.48 (1)
47.2			2.68 (2)	
45.2		5.58 (1)		3.89 (1)
44.2	1.18 (3)			
42.2			2.46 (2)	
40.2				4.19 (1)
37.2			2.38 (2)	
35.2		5.78 (1)		4.44 (1)
34.2	1.05 (3)			
32.2			2.32 (2)	
30.2				4.67 (1)
25.2		6.00 (1)		
24.2	9.11 (2)			
22.2			2.42 (2)	
20.2				5.10 (1)
15.2		6.34 (1)		
14.2	8.56 (2)			
12.2			2.41 (2)	
10.2				5.35
5.2		6.34 (1)		
4.2	7.93 (2)			
2.2			2.44 (2)	
0.2				5.48 (1)
4.8		6.33 (1)		
5.8	8.25 (2)			
14.8		6.18 (1)		
15.8	8.48 (2)			
24.8		5.90 (1)		
25.8	9.10 (2)			
34.8		5.66 (1)		
35.8	1.04 (3)			
44.8		5.42 (1)		
45.8	1.23 (3)			
49.8		5.58 (1)		
54.8		5.74 (1)		
55.8	1.71 (3)			
59.8		5.85 (1)		
60.8	2.02 (2)			
64.8		5.41 (1)		
65.8	1.99 (3)			
69.8 N		4.62 (1)		

[a] Traverses within horizontal midplane of configuration.
[b] 4 cm behind upper pin layer without boral.
[c] 4.3 cm behind upper pin layer.
[d] 5 cm behind upper pin layer with boral.
[e] Read: 1.35×10^{-2}.

Table 22. Bonner ball horizontal traverses close behind successive layers of mockup[a] (Items II B-D, reference pin pattern)

Distance from Centerline (cm)	Bonner ball count rates ($s^{-1}W^{-1}$)					
	Reflector layer, Item II B		Crossover layer, Item II C		Follow-on layer, Item II D	
	Bare counter[b]	Cd-covered counter[c]	Bare counter[d]	Cd-covered counter[d]	Bare counter[e]	Cd-covered counter[e]
70.2 S	5.17 (1)[f]	3.23 (0)		2.45 (-1)		
				2.52 (-1)		
70			2.71 (1)		1.13 (1)	4.59 (-2)
60.2	5.80 (1)	4.88 (0)				
60			4.18 (1)	4.64 (-1)	1.88 (1)	9.40 (-2)
				4.73 (-1)		
55.2	6.22 (1)					
55			5.10 (1)	6.99 (-1)		
50.2	6.88 (1)	7.30 (0)				
50			7.47 (1)	1.21 (0)	3.61 (1)	2.73 (-1)
				1.25 (0)		
45.2	7.51 (1)					
45			1.20 (2)	2.59 (0)	6.55 (1)	8.0. (-1)
				2.76 (0)		
40.2	7.96 (1)	9.30 (0)				
40			1.39 (2)	3.34 (0)	7.80 (1)	9.58 (-1)
				3.39 (0)		
35.2	8.21 (1)					
35			1.45 (2)	3.53 (0)	8.21 (1)	9.55 (-1)
30.2	8.76 (1)	1.11 (1)				
30			1.38 (2)	3.26 (0)	7.57 (1)	9.07 (-1)
				3.36 (0)		
25			1.07 (2)	2.44 (0)	5.60 (1)	4.87 (-1)
				2.38 (0)		
20.2	9.33 (1)	1.21 (1)				
20			8.45 (1)	1.52 (0)	3.84 (1)	2.41 (-1)
				1.50 (0)		
15			8.55 (1)	1.40 (0)	3.39 (1)	1.75 (-1)
10.2	1.00 (2)	1.28 (1)		1.39 (0)		
10			1.09 (2)	1.75 (0)	3.22 (1)	1.55
				1.74 (0)		
5			1.36 (2)	2.23 (0)	3.21 (1)	1.41 (-1)
				2.28 (0)		
0.2	9.69 (1)	1.23 (1)				
0			1.44 (2)	2.45 (0)	3.15 (1)	1.38 (-1)
5			1.36 (2)	2.32 (0)	3.18 (1)	1.41 (-1)
9.8	9.82 (1)	1.27 (1)				
10			1.04 (2)	1.79 (0)	3.24 (1)	1.57 (-1)
15			8.46 (1)	1.42 (0)	3.39 (1)	1.87 (-1)
19.8	9.24 (1)	1.21 (1)				
20			8.44 (1)	1.51 (0)	3.87 (1)	2.56 (-1)
25			1.09 (2)	2.28 (0)	5.75 (1)	6.01 (-1)
27.5						8.33 (-1)
29.8	8.54 (1)	1.11 (1)				
30			1.39 (2)	3.27 (0)	7.60 (1)	9.22 (-1)
35			1.44 (2)	3.52 (0)	8.12 (1)	9.65 (-1)
39.8	7.77 (1)	9.20 (0)				
40			1.36 (2)	3.40 (0)	7.74 (1)	9.24 (-1)
42.5						8.71 (-1)
45			1.08 (2)	2.75 (0)	6.14 (1)	6.94 (-1)
49.8	6.63 (1)	7.10 (0)				
50			6.71 (1)	1.77 (0)	3.44 (1)	2.37 (-1)
55			4.89 (1)	6.83 (-1)		
59.8	5.17 (1)	4.57 (0)				
60			3.91 (1)	4.66 (-1)	1.76 (1)	8.26 (-2)
69.8	4.22 (1)	2.86 (0)				
70 N			2.56 (1)	2.49 (-1)	1.05 (1)	3.65 (-2)

[a] Traverses within horizontal midplane of configurations.
[b] 4.1 cm behind reflector layer.
[c] 4 cm behind reflector layer.
[d] 4 cm behind cross-over layer.
[e] 4.2 cm behind follow-on layer.
[f] Read: 5.17×10^{1}

Table 23. Bonner ball horizontal traverses 30 cm beyond reflector layer[a] (Item II B, reference pin pattern)

Distance from Centerline (cm)	Bonner ball count rates ($s^{-1}W^{-1}$)			
	Bare counter	Cd-covered counter	5-in.-diam ball	10-in.-diam ball
70.2 S	3.94 (1)[b]	3.07 (0)	5.95 (1)	1.99 (1)
60.2	4.42 (1)	3.94 (0)	7.58 (1)	2.58 (1)
50.2	5.00 (1)	4.83 (0)	9.68 (1)	3.28 (1)
40.2	5.65 (1)	5.75 (0)	1.17 (2)	3.96 (1)
30.2	5.94 (1)	6.61 (0)	1.34 (2)	4.50 (1)
20.2	6.31 (1)	7.17 (0)	1.47 (2)	4.92 (1)
10.2	6.44 (1)	7.54 (0)	1.56 (2)	5.15 (1)
0.2	6.39 (1)	7.56 (0)	1.56 (2)	5.16 (1)
9.8	6.35 (1)	7.54 (0)	1.55 (2)	5.16 (1)
19.8	6.10 (1)	7.09 (0)	1.50 (2)	4.99 (1)
29.8	5.70 (1)	6.50 (0)	1.34 (2)	4.52 (1)
39.8	5.16 (1)	5.70 (0)	1.18 (2)	3.96 (1)
49.8	4.56 (1)	4.73 (0)	9.58 (1)	3.21 (1)
59.8	3.83 (1)	3.74 (0)	7.37 (1)	2.52 (1)
69.8 N	3.23 (1)	2.81 (0)	5.64 (1)	1.88 (1)

[a]Traverses within horizontal midplane of configuration.
[b]Read: 3.94×10^{1}.

Table 24. Bonner ball horizontal traverses within 15-cm-thick voids behind reflector and crossover layers[a] (Items II BB, CC; reference pin pattern)

Distance from Centerline (cm)	Bonner ball count rates ($s^{-1}W^{-1}$)			
	Behind reflector layer, Item II BB		Behind crossover layer, Item II CC	
	Bare counter[b]	Cd-covered counter[b]	Bare counter[c]	Cd-covered counter[c]
70 S	2.80 (2)[d]	1.09 (1)	1.37 (2)	
69.5				1.11 (0)
60	3.55 (2)	1.60 (1)	1.97 (2)	
59.5				1.73 (0)
50	4.24 (2)	2.10 (1)	2.66 (2)	
49.5				3.06 (0)
45			3.12 (2)	
44.5				4.61 (0)
40	4.77 (2)	2.52 (1)	3.44 (2)	
39.5				5.28 (0)
35			3.64 (2)	
34.5				5.43 (0)
30	5.19 (2)	2.96 (1)	3.57 (2)	
29.5				5.34 (0)
25			3.57 (2)	
24.5				4.53 (0)
20	5.76 (2)	3.30 (1)	3.59 (2)	
19.5				4.00 (0)
15			3.70 (2)	
14.5				4.06 (0)
10	6.07 (2)	3.58 (1)	3.86 (2)	
9.5				4.42 (0)
5			4.13 (2)	
4.5				4.87 (0)
0	6.11 (2)	3.55 (1)	4.22 (2)	
0.5				4.92 (0)
5			4.14 (2)	
5.5				4.83 (0)
10	6.04 (2)	3.54 (1)	3.89 (2)	
10.5				4.46 (0)
15			3.61 (2)	
15.5				4.41 (0)
20	5.54 (2)	3.30 (1)	3.56 (2)	
20.5				4.05 (0)
25			3.52 (2)	
25.5				4.67 (0)
30	5.09 (2)	2.93 (1)	3.57 (2)	
30.5				5.42 (0)
35			3.50 (2)	
35.5				5.42 (0)
40	4.54 (2)	2.52 (1)	3.41 (2)	
40.5				5.09 (0)
45			3.07 (2)	
45.5				4.47 (0)
50	4.06 (2)	2.03 (1)	2.56 (2)	
50.5				2.86 (0)
60	3.27 (2)	1.52 (1)	1.92 (2)	
60.5				1.74 (0)
70	2.38 (2)	1.02 (1)	1.40 (2)	
70.5 N				1.13 (0)

[a] Traverses within horizontal midplane of configuration.
[b] 4 cm behind reflector layer.
[c] 4 cm behind cross-over layer.
[d] Read: 2.80×10^2.

Table 25. Bonner ball horizontal traverses 30 cm beyond crossover layer[a] (Item II C, reference pin pattern)

Distance from Centerline (cm)	Bonner ball count rates ($s^{-1}W^{-1}$)			
	Barc counter	Cd-covered counter	5-in.-diam ball	10-in.-diam ball
70 S	2.61 (1)[b]	3.71 (-1)	5.63 (0)	1.74 (0)
60	3.55 (1)	5.63 (-1)	8.82 (0)	2.79 (0)
50	4.62 (1)	9.01 (-1)	1.46 (1)	4.58 (0)
45			1.74 (1)	
40	5.61 (1)	1.17 (0)	1.97 (1)	6.10 (0)
35			2.08 (1)	6.43 (0)
30	6.29 (1)	1.32 (0)	2.13 (1)	6.23 (0)
25			2.03 (1)	5.86 (0)
20	6.52 (1)	1.25 (0)	1.92 (1)	5.52 (0)
15			1.81 (1)	
10	6.69 (1)	1.19 (0)	1.78 (1)	5.18 (0)
5			1.78 (1)	
0	6.76 (1)	1.19 (0)	1.77 (1)	5.21 (0)
5			1.77 (1)	
10	6.62 (1)	1.19 (0)	1.78 (1)	5.20 (0)
15			1.82 (1)	
20	6.48 (1)	1.25 (0)	1.90 (1)	5.59 (0)
25			2.05 (1)	5.90 (0)
30	6.15 (1)	1.32 (0)	2.10 (1)	6.26 (0)
35			2.04 (1)	6.32 (0)
40	5.61 (1)	1.16 (0)	1.91 (1)	6.04 (0)
45			1.68 (1)	
50	4.58 (1)	8.97 (-1)	1.39 (1)	4.50 (0)
60	3.81 (1)	5.81 (-1)	8.35 (0)	2.68 (0)
70 N	2.79 (1)	3.69 (-1)	5.32 (0)	1.67 (0)

[a]Traverses within horizontal midplane of configuration.
[b]Read: 2.61×10^{1}.

Table 26. Bonner ball horizontal traverses 30 cm beyond follow-on layer[a] (layer D) (Item II D, reference pin pattern)

Distance from Centerline (cm)	Bonner ball count rates ($s^{-1}W^{-1}$)			
	Bare counter	Cd-covered counter	5-in.-diam ball	10-in.diam ball
70 S	1.21 (1)[b]	7.20 (-2)	9.80 (-1)	2.89 (-1)
60	1.70 (1)	1.12 (-1)	1.56 (0)	5.23 (-1)
50	2.36 (1)	2.37 (-1)	3.76 (0)	1.28 (0)
45		3.38 (-1)	5.51 (0)	1.71 (0)
40	2.93 (1)	3.80 (-1)	6.57 (0)	2.05 (0)
35		3.93 (-1)	6.96 (0)	2.14 (0)
30	3.19 (1)	4.00 (-1)	6.78 (0)	1.93 (0)
25		3.40 (-1)	5.44 (0)	1.52 (0)
20	3.09 (1)	2.54 (-1)	3.87 (0)	1.15 (0)
15		2.08 (-1)	3.08 (0)	9.07 (-1)
10	2.93 (1)	1.98 (-1)	2.84 (0)	7.92 (-1)
5		1.88 (-1)	2.74 (0)	7.42 (-1)
0	2.89 (1)	1.88 (-1)	2.70 (0)	7.39 (-1)
5		1.87 (-1)	2.72 (0)	7.50 (-1)
10	2.92 (1)	1.95 (-1)	2.85 (0)	8.02 (-1)
15		2.09 (-1)	3.09 (0)	9.19 (-1)
20	3.07 (1)	2.54 (-1)	3.85 (0)	1.16 (0)
25		3.39 (-1)	5.32 (0)	1.57 (0)
30	3.18 (1)	3.86 (-1)	6.67 (0)	1.94 (0)
35		3.84 (-1)	6.78 (0)	2.13 (0)
40	2.87 (1)	3.61 (-1)	6.42 (0)	2.02 (0)
45		3.21 (-1)	5.36 (0)	1.66 (0)
50	2.30 (1)	2.23 (-1)	3.62 (0)	1.19 (0)
60	1.63 (1)	1.03 (-1)	1.50 (0)	4.95 (-1)
70 N	1.16 (1)	6.50 (-2)	9.39 (-1)	2.81 (-1)

[a]Traverses within horizontal midplane of configuration.
[b]Read: 1.21×10^{1}.

Table 27. Bonner ball traverses along axis of large outer coolant hole (Item II D, reference pin pattern)

Distance from Reflector Layer (cm)	Bonner ball count rates ($s^{-1}W^{-1}$)	
	Bare counter	Cd-covered counter
4		3.40 (1)[a]
4.7	1.07 (3)	
6.7	1.06 (3)	
9		2.87 (1)
9.7	1.04 (3)	
14		2.38 (1)
14.7	9.68 (2)	
19.7	9.10 (2)	
24		1.55 (1)
24.7	8.57 (2)	
34		1.01 (1)
34.7	6.79 (2)	
39.7	6.22 (2)	
44		6.72 (0)
54		4.48 (0)
54.7	4.07 (2)	
64		2.79 (0)
64.7	2.73 (2)	
74		1.55 (0)
74.7	1.41 (2)	
84		7.94 (-1)
84.7	6.72 (1)	
89		6.30 (-1)
94		5.14 (-1)
94.7	4.19 (1)	
104		3.87 (-1)
104.7	3.22 (1)	
114		3.14 (-1)
114.7	2.62 (1)	

[a]Read: 3.40×10^{1}.

Table 28. Fast-neutron fluxes (>0.8 MeV) on centerline 125.5 cm beyond boron pin layer (Item III A, full pin pattern): Run 7835B

Neutron energy (MeV)	Flux (neutrons cm^{-2} MeV^{-1} kW^{-1} s^{-1})		Neutron energy (MeV)	Flux (neutrons cm^{-2} MeV^{-1} kW^{-1} s^{-1})	
	Lower limit	Upper limit		Lower limit	Upper limit
8.1135E−01[a]	6.2674E+03	6.3560E+03	5.9380E+00	1.6672E+02	1.7364E+02
9.0694E−01	6.8954E+03	6.9448E+03	6.2542E+00	1.5215E+02	1.6123E+02
1.0066E+00	6.2502E+03	6.2864E+03	6.5557E+00	1.4437E+02	1.5189E+02
1.1069E+00	5.3108E+03	5.3461E+03	6.8390E+00	1.3147E+02	1.3671E+02
1.2047E+00	4.4204E+03	4.4510E+03	7.2352E+00	1.0134E+02	1.0553E+02
1.3096E+00	3.6219E+03	3.6499E+03	7.7365E+00	6.0889E+01	6.5449E+01
1.4121E+00	3.0652E+03	3.0926E+03	8.2364E+00	3.9780E+01	4.3758E+01
1.5107E+00	2.6900E+03	2.7156E+03	8.7578E+00	3.2084E+01	3.4883E+01
1.6100E+00	2.3990E+03	2.4213E+03	9.2613E+00	2.6209E+01	2.8616E+01
1.7095E+00	2.1265E+03	2.1474E+03	9.7411E+00	2.0060E+01	2.2322E+01
1.8125E+00	1.8482E+03	1.8685E+03	1.0259E+01	1.3182E+01	1.5135E+01
1.9323E+00	1.5644E+03	1.5837E+03	1.0777E+01	8.7908E+00	1.0506E+01
2.1000E+00	1.2384E+03	1.2561E+03	1.1247E+01	7.3614E+00	8.9344E+00
2.2961E+00	9.1970E+02	9.3682E+02	1.1751E+01	6.5629E+00	7.9443E+00
2.4988E+00	6.8534E+02	6.9895E+02	1.2393E+01	5.1858E+00	6.4054E+00
2.7026E+00	5.2303E+02	5.3803E+02	1.3201E+01	4.1407E+00	4.9936E+00
2.8984E+00	4.1845E+02	4.3303E+02	1.4021E+01	3.1383E+00	3.7566E+00
3.0975E+00	3.3414E+02	3.5000E+02	1.4792E+01	1.7736E+00	2.2590E+00
3.2965E+00	2.7897E+02	2.9136E+02	1.5629E+01	5.1764E−01	9.3994E−01
3.5009E+00	2.4190E+02	2.5696E+02	1.6539E+01	−5.8188E−02	2.8544E−01
3.7074E+00	2.1851E+02	2.3064E+02	1.7533E+01	−2.2137E−01	1.0930E−01
3.9061E+00	2.1195E+02	2.2247E+02	1.8521E+01	−2.4941E−01	1.3162E−01
4.1528E+00	2.1868E+02	2.2928E+02	1.9498E+01	−2.0212E−01	1.6696E−01
4.4540E+00	2.2961E+02	2.3880E+02	2.0556E+01	−1.9208E−01	1.7809E−01
4.7521E+00	2.3823E+02	2.4708E+02	2.1580E+01	−1.4427E−01	2.1025E−01
5.0422E+00	2.2927E+02	2.3710E+02	2.2560E+01	−1.7166E−01	1.9273E−01
5.3459E+00	2.0979E+02	2.1723E+02	2.3471E+01	−1.8428E−01	2.0947E−01
5.6453E+00	1.8824E+02	1.9634E+02			

E1 (MeV)	E2 (MeV)	Integral (neutrons cm^{-2} kW^{-1} s^{-1})	Error (neutrons cm^{-2} kW^{-1} s^{-1})
0.811	1.000	1.2687E+03	4.8892E+00
1.000	1.200	1.0794E+03	3.4673E+00
1.200	1.600	1.2974E+03	5.4126E+00
1.600	2.000	7.6289E+02	4.0735E+00
2.000	3.000	7.6585E+02	7.8396E+00
3.000	4.000	2.6424E+02	6.5570E+00
4.000	6.000	4.3589E+02	8.4990E+00
6.000	8.000	2.3119E+02	5.8050E+00
8.000	10.000	6.2364E+01	2.8430E+00
10.000	12.000	1.9818E+01	1.6617E+00
12.000	16.000	1.3353E+01	1.4358E+00
16.000	20.000	4.0500E−02	7.1617E−01
1.500	15.000	2.8124E+03	3.9730E+01
3.000	12.000	1.0124E+03	2.5371E+01

[a]Read: 8.1135 × 10^{-1}.

Table 29. Neutron fluxes (50 keV to 1.4 MeV) on centerline 125.5 cm beyond boron pin layer (Item III A, full pin pattern): Runs 1511A, 1510A, and 1509B

N	Energy boundary (MeV)		Flux (neutron cm^{-2} MeV^{-1} kW^{-1} s^{-1})	Error (%)
1	0.0453	0.0529	6.49E 04	4.48
2	0.0529	0.0642	4.86E 04	4.49
3	0.0642	0.0736	5.93E 04	5.20
4	0.0736	0.0869	6.09E 04	3.92
5	0.0869	0.1038	3.72E 04	5.50
6	0.1038	0.1208	4.30E 04	5.58
7	0.1208	0.1435	5.50E 04	3.49
8	0.1435	0.1680	4.24E 04	4.67
9	0.1680	0.1983	3.70E 04	4.68
10	0.1983	0.2322	2.95E 04	5.75
1	0.1672	0.1980	3.70E 04	1.94
2	0.1980	0.2332	2.78E 04	2.53
3	0.2332	0.2728	2.73E 04	2.58
4	0.2728	0.3212	3.22E 04	1.94
5	0.3212	0.3784	2.87E 04	1.96
1	0.2718	0.3262	3.23E 04	0.70
2	0.3262	0.3806	2.61E 04	0.96
3	0.3806	0.4440	1.79E 04	1.30
4	0.4440	0.5256	1.55E 04	1.27
5	0.5256	0.6162	1.78E 04	1.08
6	0.6162	0.7249	1.70E 04	0.96
7	0.7249	0.8608	1.0 E 04	1.27
8	0.8608	1.0058	8.22. 03	1.58
9	1.0058	1.1871	6.35E 03	1.60
10	1.1871	1.3955	4.52E 03	1.94

Table 30. Bonner ball horizontal traverses 30 cm beyond boron pin layer[a] (Item III A, full pin pattern)

Distance from Centerline (cm)	Bonner ball count rates (s^{-1} W^{-1})			
	Bare counter	Cd-covered counter	5-in.-diam ball	10-in.diam ball
70 S	4.36 (2)[b]	1.05 (1)	2.63 (2)	1.02 (2)
60	4.43 (2)	1.12 (1)	3.31 (2)	1.33 (2)
50	4.22 (2)	1.17 (1)	3.97 (2)	1.66 (2)
40	3.75 (2)	1.11 (1)	4.57 (2)	2.00 (2)
30	3.21 (2)	1.01 (1)	5.07 (2)	2.29 (2)
20	2.81 (2)	9.46 (0)	5.41 (2)	2.48 (2)
10	2.59 (2)	9.03 (0)	5.56 (2)	2.56 (2)
0	2.44 (2)	8.66 (0)	5.56 (2)	2.62 (2)
10	2.58 (2)	9.03 (0)	5.52 (2)	2.54 (2)
20	2.73 (2)	9.26 (0)	5.30 (2)	2.45 (2)
30	3.11 (2)	1.02 (1)	5.00 (2)	2.26 (2)
40	3.65 (2)	1.08 (1)	4.48 (2)	1.92 (2)
50	4.02 (2)	1.09 (1)	3.87 (2)	1.62 (2)
60	4.21 (2)	1.05 (1)	3.16 (2)	1.30 (2)
70 N	4.04 (2)	9.66 (0)	2.54 (2)	9.80 (1)

[a]Traverses within horizontal midplane of configuration.
[b]Read: 4.36×10^2.

Table 31. Bonner ball horizontal traverses close behind boron pin with and without boral shroud[a] (Items III A, AA; full pin pattern)

Distance from Centerline (cm)	Bonner ball count rates (s^{-1} W^{-1})			
	Without boral shroud		With boral shroud	
	Bare counter[b]	Cd-covered counter[c]	Bare counter[d]	Cd-covered counter[d]
70 S	7.51 (2)[e]	1.89 (1)	3.96 (1)	4.26 (0)
65	7.99 (2)	2.11 (1)		
60	6.91 (2)	2.07 (1)	2.89 (1)	5.30 (0)
55	4.97 (2)	1.65 (1)	4.57 (1)	5.89 (0)
50	2.95 (2)	1.14 (1)	8.19 (1)	6.86 (0)
47.5				6.64 (0)
45			6.08 (1)	6.27 (0)
40	1.44 (2)	8.19 (0)	4.71 (1)	6.09 (0)
30	1.04 (2)	7.46 (0)	3.37 (1)	6.23 (0)
20	9.27 (1)	7.85 (0)	3.01 (1)	6.44 (0)
10	8.66 (1)	7.98 (0)	2.99 (1)	6.62 (0)
0	8.72 (1)	7.96 (0)	2.68 (1)	6.48 (0)
10	8.74 (1)	7.88 (0)	2.88 (1)	6.72 (0)
20	9.52 (1)	7.53 (0)		
30	1.10 (2)	7.26 (0)		
40	1.54 (2)	7.73 (0)		
50	3.34 (2)	1.13 (1)		
55	5.38 (2)	1.53 (1)		
60	7.13 (2)	1.90 (1)		
65	7.82 (2)	1.91 (1)		
70 N	7.43 (2)	1.66 (1)		

[a]Traverses within horizontal midplane of configuration.
[b]4.2 cm behind upper pin layer.
[c]4 cm behind upper pin layer.
[d]5.6 cm behind upper pin layer.
[e]Read: 7.51×10^2.

Table 32. Bonner ball horizontal traverses within 15-cm-thick void between boron pin layer and reflector layer with and without boral shroud[a] (Items III AAA, AAAA; full pin pattern)

Distance from Centerline (cm)	Bonner ball count rates (s^{-1} W^{-1})			
	Without boral shroud		With boral shroud	
	Bare counter[b]	Cd-covered counter[c]	Bare counter[d]	Cd-covered counter[d]
70 S	1.59 (3)[e]	3.81 (1)	8.68 (1)	1.22 (1)
65	1.61 (3)	4.38 (1)	8.00 (1)	1.43 (1)
60	1.61 (3)	4.49 (1)	8.46 (1)	1.64 (1)
55		4.21 (1)	1.13 (2)	1.84 (1)
50	1.09 (3)	3.72 (1)	1.60 (2)	2.15 (1)
45			1.35 (2)	2.16 (1)
40	8.21 (2)	3.37 (1)	1.24 (2)	2.27 (1)
35				2.36 (1)
30	6.56 (2)	3.27 (1)	1.16 (2)	2.44 (1)
20	5.51 (2)	3.28 (1)	1.15 (2)	2.63 (1)
10	4.97 (2)	3.32 (1)	1.14 (2)	2.72 (1)
0	5.12 (2)	3.38 (1)	1.14 (2)	2.82 (1)
10	5.10 (2)	3.29 (1)	1.11 (2)	2.71 (1)
20	5.62 (2)	3.29 (1)		
30	6.51 (2)	3.26 (1)		
40	8.08 (2)	3.37 (1)		
50	1.13 (3)	3.84 (1)		
55	1.38 (3)	4.27 (1)		
60	1.63 (3)	4.40 (1)		
65	1.67 (3)	4.19 (1)		
70 N		3.66 (1)		

[a]Traverses within horizontal midplane of configuration.
[b]4.7 cm behind upper pin layer.
[c]5 cm behind upper pin layer.
[d]4.5 cm behind upper pin layer.
[e]Read: 1.59×10^3.

Table 33. Bonner ball horizontal traverses close behind successive layers of mockup[a] (Items III B-D, full pin pattern)

Distance from Centerline (cm)	Bonner ball count rates (s^{-1} W^{-1})					
	Reflector layer, Item III B		Crossover layer, Item III C		Follow-on layer, Item III D	
	Bare counter[b]	Cd-covered counter[b]	Bare counter[c]	Cd-covered counter[c]	Bare counter[d]	Cd-covered counter[d]
70 S	3.62 (1)[f]	2.61 (0)	2.16 (1)	2.27 (-1)	8.82 (0)	4.21 (-2)
60	3.81 (1)	4.00 (0)	3.15 (1)	4.23 (-1)	1.48 (1)	8.61 (-2)
55			3.96 (1)	6.33 (-1)	1.90 (1)	1.29 (-1)
50	4.45 (1)	5.52 (0)	5.42 (1)	1.10 (0)	2.84 (1)	2.33 (-1)
45			8.64 (1)	2.34 (0)	5.19 (1)	6.54 (-1)
40	4.70 (1)	6.63 (0)	1.04 (2)	2.84 (0)	6.07 (1)	8.10 (-1)
35			1.07 (2)	2.94 (0)	6.34 (1)	8.26 (-1)
30	4.91 (1)	7.49 (0)	1.01 (2)	2.72 (0)	5.98 (1)	7.94 (-1)
25			7.95 (1)	1.94 (0)	4.34 (1)	4.66 (-1)
20	5.12 (1)	8.11 (0)	6.21 (1)	1.26 (0)	2.92 (1)	2.19 (-1)
15			6.21 (1)	1.21 (0)	2.58 (1)	1.62 (-1)
10	5.40 (1)	8.61 (0)	7.83 (1)	1.53 (0)	2.48 (1)	1.40 (-1)
5			9.72 (1)	1.97 (0)	2.45 (1)	1.27 (-1)
0	5.26 (1)	8.28 (0)	1.04 (2)	2.13 (0)	2.43 (1)	1.28 (-1)
5			9.79 (1)	2.00 (0)	2.45 (1)	1.31 (-1)
10	5.33 (1)	8.41 (0)	7.75 (1)	1.51 (0)	2.48 (1)	1.36 (-1)
15			6.27 (1)	1.18 (0)	2.58 (1)	1.61 (-1)
20	5.00 (1)	7.87 (0)	6.16 (1)	1.24 (0)	2.94 (1)	2.10 (-1)
25			7.87 (1)	1.92 (0)	4.24 (1)	4.34 (-1)
30	4.77 (1)	7.24 (0)	9.88 (1)	2.70 (0)	5.86 (1)	7.59 (-1)
35			1.05 (2)	2.86 (0)	6.19 (1)	8.09 (-1)
40	4.44 (1)	6.26 (0)	1.00 (2)	2.75 (0)	5.97 (1)	7.94 (-1)
45			8.15 (1)	2.21 (0)	4.92 (1)	6.48 (-1)
50	4.15 (1)	4.99 (0)	5.07 (1)	1.04 (0)	2.74 (1)	2.23 (-1)
55			3.75 (1)	5.93 (-1)	1.83 (1)	1.20 (-1)
60	3.47 (1)	3.46 (0)	3.04 (1)	4.20 (-1)	1.38 (1)	7.55 (-2)
70 N	3.18 (1)	2.34 (0)	2.16 (1)	2.26 (-1)	8.68 (0)	3.72 (-2)

[a] Traverses within horizontal midplane of configuration.
[b] 4 cm behind reflector layer.
[c] 4 cm behind crossover layer.
[d] 4.3 cm behind layer D.
[e] 4 cm behind follow-on layer.
[f] Read: 3.62×10^{1}.

Table 34. Bonner ball horizontal traverses 30 cm beyond reflector layer[a] (Item III B, full pin pattern)

Distance from Centerline (cm)	Bonner ball count rates (s^{-1} W^{-1})			
	Bare counter	Cd-covered counter	5-in.-diam ball	10-in.-diam ball
70 S	2.52 (1)[b]	2.30 (0)	5.13 (1)	1.86 (1)
60	2.82 (1)	2.91 (0)	6.60 (1)	2.41 (1)
50	3.13 (1)	3.61 (0)	8.49 (1)	3.08 (1)
40	3.39 (1)	4.18 (0)	9.99 (1)	3.69 (1)
30	3.59 (1)	4.65 (0)	1.16 (2)	4.22 (1)
20	3.73 (1)	4.97 (0)	1.26 (2)	4.53 (1)
10	3.81 (1)	5.24 (0)	1.32 (2)	4.75 (1)
0	3.77 (1)	5.22 (0)	1.31 (2)	4.76 (1)
10	3.74 (1)	5.18 (0)	1.29 (2)	4.70 (1)
20	3.65 (1)	4.92 (0)	1.25 (2)	4.50 (1)
30	3.46 (1)	4.56 (0)	1.12 (2)	4.12 (1)
40	3.23 (1)	4.03 (0)	9.74 (1)	3.60 (1)
50	2.95 (1)	3.41 (0)	7.98 (1)	2.96 (1)
60	2.58 (1)	2.75 (0)	6.36 (1)	2.33 (1)
70 N	2.26 (1)	2.14 (0)	4.85 (1)	1.76 (1)

[a]Traverses within horizontal midplane of configuration.
[b]Read: 2.52×10^{1}.

Table 35. Bonner ball horizontal traverses within 15-cm-thick voids behind reflector and crossover layers[a] (Items III BB, CC; full pin pattern)

Distance from Centerline (cm)	Bonner ball count rates (s^{-1} W^{-1})			
	Behind reflector layer, Item III BB		Behind crossover layer, Item III CC	
	Bare counter[b]	Cd-covered counter[b]	Bare counter[c]	Cd-covered counter[d]
70 S	1.80 (2)[e]	8.33 (0)	1.04 (2)	9.72 (-1)
60	2.38 (2)	1.22 (1)	1.48 (2)	1.57 (0)
55			1.71 (2)	1.93 (0)
50	2.82 (2)	1.59 (1)	1.97 (2)	2.61 (0)
45			2.33 (2)	3.74 (0)
40	3.10 (2)	1.86 (1)	2.58 (2)	4.24 (0)
35			2.69 (2)	4.44 (0)
30	3.37 (2)	2.13 (1)	2.70 (2)	4.37 (0)
25			2.65 (2)	3.84 (0)
20	3.64 (2)	2.35 (1)	2.64 (2)	3.47 (0)
15			2.76 (2)	3.54 (0)
10	3.89 (2)	2.52 (1)	2.93 (2)	3.84 (0)
5			3.07 (2)	4.16 (0)
0	3.95 (2)	2.54 (1)	3.18 (2)	4.28 (0)
5			3.03 (2)	4.14 (0)
10	3.84 (2)	2.49 (1)	2.86 (2)	3.78 (0)
15			2.69 (2)	3.51 (0)
20	3.64 (2)	2.32 (1)	2.62 (2)	3.48 (0)
25			2.63 (2)	3.89 (0)
30	3.29 (2)	2.08 (1)	2.65 (2)	4.32 (0)
35			2.67 (2)	4.31 (0)
40	3.00 (2)	1.82 (1)	2.47 (2)	4.05 (0)
45			2.26 (2)	3.52 (0)
50	2.71 (2)	1.54 (1)	1.92 (2)	2.45 (0)
55			1.69 (2)	1.86 (0)
60	2.23 (2)	1.18 (1)	1.48 (2)	1.50 (0)
70 N	1.67 (2)	7.96 (0)	1.05 (2)	9.50 (-1)

[a] Traverses within horizontal midplane of configuration.
[b] 4 cm behind reflector layer.
[c] 4 cm behind crossover layer.
[d] 4.4 cm behind crossover layer.
[e] Read: 1.80×10^2.

Table 36. Bonner ball horizontal traverses 30 cm beyond crossover layer[a] (Item III CC; full pin pattern)

Distance from Centerline	Bonner ball count rates (s^{-1} W^{-1})			
	Bare counter	Cd-covered counter	5-in.-diam ball	10-in.-diam ball
70 S	2.07 (1)[b]	3.28 (-1)	5.41 (0)	1.63 (0)
60	2.74 (1)	4.94 (-1)	8.51 (0)	2.61 (0)
50	3.52 (1)	7.48 (-1)	1.34 (1)	4.36 (0)
45			1.59 (1)	
40	4.19 (1)	9.71 (-1)	1.77 (1)	5.69 (0)
35			1.88 (1)	5.96 (0)
30	4.66 (1)	1.09 (0)	1.89 (1)	5.86 (0)
25			1.83 (1)	5.54 (0)
20	4.81 (1)	1.04 (0)	1.70 (1)	5.17 (0)
15			1.64 (1)	
10	4.98 (1)	1.00 (0)	1.62 (1)	4.87 (0)
0	4.94 (1)	9.98 (-1)	1.61 (1)	4.92 (0)
10	4.89 (1)	1.01 (0)	1.61 (1)	4.82 (0)
20	4.72 (1)	1.03 (0)	1.73 (1)	5.08 (0)
25		1.07 (0)	1.81 (1)	5.43 (0)
30	4.54 (1)	1.06 (0)	1.87 (1)	5.72 (0)
35		1.01 (0)	1.81 (1)	5.79 (0)
40	4.04 (1)	9.42 (-1)	1.67 (1)	5.51 (0)
45			1.48 (1)	
50	3.32 (1)	7.30 (-1)	1.22 (1)	4.12 (0)
60	2.65 (1)	4.87 (-1)	7.54 (0)	2.56 (0)
70 N	1.98 (1)	3.10 (-1)	4.90 (0)	1.58 (0)

[a]Traverses within horizntal midplane of configuration.
[b]Read: 2.07×10^{1}.

Table 37. Bonner ball horizontal traverses 30 cm beyond follow-on layer[a] (layer D) (Item III D, full pin pattern)

Distance from Centerline	Bonner ball count rates (s^{-1} W^{-1})			
	Bare counter	Cd-covered counter	5-in.-diam ball	10-in.-diam ball
70 S	9.92 (0)[b]	6.71 (-2)	9.66 (-1)	3.04 (-1)
60	1.37 (1)	1.00 (-1)	1.51 (0)	5.37 (-1)
55	1.61 (1)	1.33 (-1)	2.11 (0)	8.10 (-1)
50	1.88 (1)	1.07 (-1)	3.32 (0)	1.24 (0)
45	2.12 (1)	2.80 (-1)	4.85 (0)	1.70 (0)
40	2.30 (1)	3.20 (-1)	5.76 (0)	2.00 (0)
35	2.41 (1)	3.24 (-1)	6.09 (0)	2.10 (0)
30	2.52 (1)	3.33 (-1)	5.97 (0)	1.97 (0)
25	2.50 (1)	2.98 (-1)	4.91 (0)	1.53 (0)
20	2.42 (1)	2.29 (-1)	3.53 (0)	1.18 (0)
15	2.36 (1)	1.96 (-1)	2.91 (0)	9.13 (-1)
10	2.32 (1)	1.81 (-1)	2.67 (0)	8.02 (-1)
5	2.30 (1)	1.74 (-1)	2.56 (0)	7.61 (-1)
0	2.27 (1)	1.74 (-1)	2.52 (0)	7.42 (-1)
5	2.29 (1)	1.71 (-1)	2.54 (0)	7.60 (-1)
10	2.31 (1)	1.78 (-1)	2.60 (0)	7.79 (-1)
15	2.35 (1)	1.90 (-1)	2.82 (0)	8.90 (-1)
20	2.42 (1)	2.20 (-1)	3.38 (0)	1.14 (0)
25	2.49 (1)	2.78 (-1)	4.61 (0)	1.44 (0)
30	2.48 (1)	3.26 (-1)	5.74 (0)	1.79 (0)
35	2.40 (1)	3.14 (-1)	5.89 (0)	2.01 (0)
40	2.28 (1)	2.98 (-1)	5.59 (0)	1.98 (0)
45	2.09 (1)	2.74 (-1)	4.76 (0)	1.64 (0)
50	1.82 (1)	2.01 (-1)	3.30 (0)	1.19 (0)
55	1.57 (1)	1.36 (-1)	2.09 (0)	7.87 (-1)
60	1.33 (1)	1.04 (-1)	1.47 (0)	5.26 (-1)
70 N	9.79 (0)	6.51 (-2)	9.39 (-1)	2.91 (-1)

[a]Traverses within horizontal midplane of configuration.
[b]Read: 9.92×10^{0}.

Table 38. Bonner ball traverses along axis of large coolant hole (Item III D, full pin pattern)

Distance from reflector layer (cm)	Bonner ball count rates (s^{-1} W^{-1})	
	Bare counter	Cd-covered counter
5.4		2.63 (1)[a]
5.5	7.55 (2)	
10.4		2.20 (1)
10.5	7.30 (2)	
15.4		1.85 (1)
15.5	7.03 (2)	
20.4		1.53 (1)
20.5	6.54 (2)	
25.4		1.23 (1)
25.5	6.16 (2)	
35.4		8.26 (0)
35.5	5.17 (2)	
45.4		5.48 (0)
45.5	4.02 (2)	
55.4		3.63 (0)
55.5	2.98 (2)	
65.4		2.27 (0)
65.5	1.96 (2)	
75.4		1.21 (0)
75.5	9.80 (1)	
80.4		8.21 (-1)
80.5	6.55 (1)	
85.4		6.21 (-1)
85.5	4.73 (1)	
90.4		4.93 (-1)
90.5	3.77 (1)	

[a]Read: 2.63×10^{1}.

APPENDIX C. LIST OF FIGURES

ORNL/TM-8977
Distribution Category UC-77

INTERNAL DISTRIBUTION

1-2. L. S. Abbott
3. D. E. Bartine
4. S. N. Cramer
5. G. F. Flanagan
6. J. L. Hull
7. L. B. Holland
8-12. D. T. Ingersoll
13. J. O. Johnson
14. P. R. Kasten
15. F. C. Maienschein
16. J. J. Manning
17. D. L. Moses
18. F. R. Mynatt
19-23. F. J. Muckenthaler
24. J. W. Paul
25. R. W. Peelle
26. C. O. Slater
27. D. R. Vondy
28. L. R. William
29. A. Zucker
30. P. W. Dickson, Jr. (Consultant)
31. Professor Gene H. Golub (Consultant)
32. H. J. C. Kouts (Consultant)
33. D. Steiner (Consultant)
34-35. Central Research Library
36. EPMD Reports Office
37. Y-12 Technical Library Document Reference Section
38-39. Laboratory Records Department
40. Laboratory Records ORNL, RC
41. ORNL Patent Office

EXTERNAL DISTRIBUTION

42-43. R. Ng, Division of HTR Development, DOE, NE-15, Washington, D.C. 20545
44. Office of Assistant Manager for Energy Research and Development, DOE-ORO, P.O. Box E, Oak Ridge, TN 37830 Attention: S. W. Ahrends/M. Rohr
45. Director, Office of Converter Reactor Deployment, DOE, NE-10, Washington, D.C. 20545
46. J. E. Fox, Division of HTR Development, DOE, NE-15, Washington, D.C. 20545
47. L. Lanni, DOE-SAN, 1333 Broadway, Oakland, CA 94612

GA Technologies, P.O. Box 81608, San Diego, CA 92138:
48. A. J. Neylan
49. S. J. Brown

Gas Cooled Reactor Associates, 10240 Sorrento Valley Rd., Suite 300, San Diego, CA 92121:
50. L. D. Mears
51. G. Jones

52. W. R. Pflasterer, General Electric, P.O. Box 508, Sunnyvale, CA 94086

53-171. For distribution as shown in TID-4500, Distribution Category UC-77 -- Gas Cooled Reactor Technology

GOVERNMENT PRINTING OFFICE: 1984-746-067/4119